1

Study of Electroweak Interactions at the Energy Frontier

Conveners: A. Kotwal and D. Wackeroth

M. Baak, A. Bodek, R. Caputo, T. Corbett, C. Degrande, O. Eboli, J. Erler, B. Feigl, A. Freitas, J. Gonzalez Fraile, C. Gonzalez-Garcia, J. Han, S. Heinemeyer, J. L. Holzbauer, S.-C. Hsu, W. Kilian, S. Li, M. Marx, O. Mattelaer, J. Metcalfe, M.-A. Pleier, C. Pollard, M. Rauch, J. Reuter, M. Rominsky, J. Rojo, W. Sakumoto, C. Schwinn, R. Sekulla, A. Vicini, G. Weiglein, G. Wilson, L. Zeune

1.1 Introduction

Authors: Ashutosh, Doreen

Particle physics research at the energy frontier has entered an exciting era: Experiments at the CERN Large Hadron Collider (LHC) are exploring the fabric of matter at an unprecedented level of precision and are expected to provide answers to some of the most fundamental questions in science. The recent discovery of a Higgs boson with SM-like properties at the LHC marks the beginning of an exciting journey with the goal to fully reveal the nature of the mechanism responsible for the generation of mass and its messenger, the Higgs boson. Besides the study of the Higgs boson at the LHC and future collider experiments, these experiments at the energy frontier strive to discover new particles and to gain new insights in the fundamental principles that govern all dynamics and properties of matter, i.e. beyond what is described by the Standard Model (SM) of particle physics.

The SM is a thoroughly tested framework for describing electromagnetic, weak and strong interactions of the fundamental constituents of matter, based on a symmetry principle and mathematically formulated as a renormalizable Quantum Field Theory. The SM successfully describes all presently observed electroweak and strong interactions of matter particles (quarks and leptons) and of the mediators of the fundamental forces (photon, W and Z bosons, and the gluon). Despite this enormous success of the SM, it is generally accepted that the SM is merely a low-energy approximation to a more fundamental theory, which is expected to reveal itself at the LHC or at future high-energy experiments, in form of the emergence of new, non-SM particles and interactions. A promising candidate for a theory beyond the SM, which also provides a dark matter candidate, is Supersymmetry (SUSY), an additional symmetry connecting fermions and bosons. The LHC is presently searching for signals of SUSY, and already succeeded in excluding a range of possible manifestations of SUSY. While direct signals of new particles (*i.e.*, the on-mass shell production of non-SM particles) may require collider energies not yet accessible, it is possible that new physics manifests itself first in form of minute deviations between measurements and equally precise predictions of properties of SM particles due to the indirect (virtual) presence of new particles in quantum-loop corrections.

This is the realm of electroweak precision physics, where well-defined electroweak precision observables (EWPO) are being measured to a high degree of precision in the interactions of W and Z bosons and are equally well predicted by complex quantum-field theoretical calculations of these quantum loop effects of SM

and beyond-the-SM (BSM) particles. The powerful concept of precision physics not only tests the SM as a full-fledged Quantum Field Theory, but also provides indirect access to currently unobserved sectors of the SM and beyond. Examples of successful applications of precision physics in the recent past include the test of the electroweak sector of the SM at the 0.1% level at LEP and the SLC [**?**], an indirect prediction of the mass of the top quark and the SM Higgs boson prior to their discovery respectively in $p\bar{p}$ collisions at the Tevatron and pp collisions at the LHC, and exclusion of, or severe constraints on, various extensions of the SM (e. g. Technicolor). In this report we will study the potential of EWPO measured at future high-energy colliders for revealing signals of new physics, constraining the parameter space of BSM models, or providing additional information about the underlying model once a new particle is discovered.

Apart from UV-complete theories such as SUSY, an alternate way to indirectly search for signals of BSM physics is based on Effective Field Theories (EFT). If the new physics scale is well above the energies reached in experiments, the new degrees of freedom cannot be produced directly and the new physics appears only as new interactions between the known particles. These new interactions are included in the Lagrangian as higher-dimensional operators which are invariant under the SM symmetries and suppressed by the new physics scale Λ,

$$\mathcal{L}_{\mathcal{EFT}} = \mathcal{L}_{SM} + \sum_{d>4} \sum_{i} \frac{c_i}{\Lambda^{d-4}} \mathcal{O}_i \tag{1.1}$$

where d is the dimension of the operators. In the limit $\Lambda \to \infty$, this EFT Lagrangian reduces to the SM one. Since the c_i are fixed by the complete high energy theory, any extension of the SM can be parametrized by this Lagrangian where the coefficients of the operators are kept as free parameters. Below the new physics scale, only the operators with lowest dimensions can give a large contribution and need to be kept. In particular, the SM contribution is expected to be the larger than the new physics one. Once truncated, the EFT Lagrangian becomes predictive even without fixing the coefficients and parametrizes any heavy new physics scenario. However, it should be kept in mind that this truncated Lagrangian is only valid below the new physics scale. Using the EFT approach we will explore the potential of multi-boson processes at the LHC and ILC for providing information about the scale of new physics.

EFT operators are a useful method of parameterizing the predictions of various strongly-interacting light Higgs (SILH) models which describe the Higgs boson as a pseudo-Goldstone Boson arising from the breaking of a larger symmetry. The lightness of the Higgs boson is the big question raised by the non-stability of the SM Higgs potential under the effect of quantum loops. While SUSY offers an elegant solution which is weakly-coupled and perturbative, EFT operators provide a starting point for exploring strongly-coupled solutions to this important question. Some of these operators induce deviations in EWPOs and Higgs couplings as well as multi-boson production, while others are uniquely probed by multi-boson production.

1.2 Electroweak precision physics

Authors: Doreen, Ashutosh

1.2.1 Uncertainties in predictions of Z pole observables, $\sin^2\theta^l_{\mathbf{eff}}$ and M_W

Author: Ayres Freitas

At e^+e^- colliders, near the Z-peak the differential cross section for $e^+e^- \to f\bar{f}$ can be written as[1]

$$\frac{d\sigma}{d\cos\theta} = \mathcal{R}_{\rm ini}\left[\frac{9}{2}\pi\,\frac{\Gamma_{ee}\Gamma_{ff}(1-\mathcal{P}_e\mathcal{A}_e)(1+\cos^2\theta)+2(\mathcal{A}_e-\mathcal{P}_e)\mathcal{A}_f\cos\theta}{(s-M_Z^2)^2-M_Z^2\Gamma_Z^2}+\sigma_{\rm non-res}\right], \tag{1.2}$$

$$\text{where}\Gamma_{ff} = \mathcal{R}_V^f g_{Vf}^2+\mathcal{R}_A^f g_{Af}^2, \qquad \Gamma_Z=\sum_f\Gamma_{ff}, \tag{1.3}$$

$$\mathcal{A}_f = 2\frac{g_{Vf}/g_{Af}}{1+(g_{Vf}/g_{Af})^2} = \frac{1-4|Q_f|\sin^2\theta_{\rm eff}^f}{1-4\sin^2\theta_{\rm eff}^f+8(\sin^2\theta_{\rm eff}^f)^2}. \tag{1.4}$$

Here Γ_Z is the total Z decay width, Γ_{ff} is the partial width for the decay $Z\to f\bar{f}$, and g_{Vf}/g_{Af} are the effective vector/axial-vector coupling that mediate this decay. These effective couplings include higher-order loop corrections to the vertex, except for QED and QCD corrections to the external $f\bar{f}$ system, which are captured by the radiator functions $\mathcal{R}_V^f$ and $\mathcal{R}_A^f$. The factor $\mathcal{R}_{\rm ini}$, on the other hand, accounts for QED radiation in the initial-state. (Specifically, as written in eq. 1.2, it describes these effects *relative* to the final-state radiation contribution for e^+e^-.)

Equation 1.2 explicitly spells out the leading Z-pole contribution, while additional effects from photon exchange and box corrections are included in the remainder $\sigma_{\rm non-res}$.

The ratio of the vector and axial vector couplings of fermions to the Z boson, g_{Vf} and g_{Af} is commonly parametrized through the effective weak mixing angle $\sin^2\theta_{\rm eff}^f$. At e^+e^- colliders it can be determined from the angular distribution of fermions in $e^+e^-\to f\bar{f}$ processes with respect to the scattering angle $\cos\theta$ or from the dependence on the initial electron polarization $\mathcal{P}_e$:

$$A_{\rm FB} \equiv \frac{\sigma(\cos\theta>0)-\sigma(\cos\theta<0)}{\sigma(\cos\theta>0)+\sigma(\cos\theta<0)} = \mathcal{R}_{\rm FB}\,\tfrac{3}{4}\mathcal{A}_e\mathcal{A}_f, \tag{1.5}$$

$$A_{\rm LR} \equiv \frac{\sigma(\mathcal{P}_e>0)-\sigma(\mathcal{P}_e<0)}{\sigma(\mathcal{P}_e>0)+\sigma(\mathcal{P}_e<0)} = \mathcal{A}_e. \tag{1.6}$$

The total cross-section, decay width Γ_Z, and branching ratios of the Z boson are measured from the rates and lineshape of the cross sections $\sigma_{e^+e^-\to f\bar{f}}(s)$ on the Z pole ($\sqrt{s}=M_Z$) and for at least one value of $\sqrt{s}$ each above and below the pole ($\sqrt{s}=M_Z\pm\Delta E$).

At hadron colliders, the effective weak mixing angle can be determined from the forward-backward asymmetry of the process $q\bar{q}\to\ell^+\ell^-$ ($\ell=e,\mu$) near the Z pole. However, one cannot determine on a event-by-event basis from which side the quark and the anitquark where coming. For a $p\bar{p}$ initial state, it is generally assumed that the (anti)quark originated from the (anti)proton, respectively, and the dilution effect from the opposite possiblity is evaluated based on Monte-Carlo simulations [54]. For a pp initial state, the boost direction of the $\ell^+\ell^-$ system is defined as the quark direction [55], based on the observation that the valence quarks from the proton tend to be more energetic than the sea antiquarks. Again, dilution effects from the wrong quark-antiquark assignment are studied with Monte-Carlo generators.

Due to the high precision of the experimental measurements for these observables, much effort has gone into their theoretical calculation within the Standard Model (SM).

The effective weak mixing angle can be written as

$$\sin^2\theta_{\rm eff}^f = \sin^2\theta_{\rm W}(1+\Delta\kappa), \tag{1.7}$$

where $\sin^2\theta_{\rm W} = 1-M_W^2/MZ^2$ is often called the *on-shell* weak mixing angle, and $\Delta\kappa$ denotes the contribution from radiative corrections.

[1] For a review, see Ref. [53].

For leptonic final states, the effective weak mixing angle $\sin^2\theta^\ell_{\rm eff}$ has been calculated to the complete two-loop order [56, 57], and 3- and 4-loop corrections of order $\mathcal{O}(\alpha\alpha_s^2)$ [58] and $\mathcal{O}(\alpha\alpha_s^3)$ [59] are also known. Furthermore, the leading $\mathcal{O}(\alpha^3)$ and $\mathcal{O}(\alpha^2\alpha_s)$ contributions for large values of m_t [60] or m_H [61] have been computed.

The current uncertainty from unknown higher orders is estimated to amount to about 4.5×10^{-5} [57], which mainly stems from missing $\mathcal{O}(\alpha^2\alpha_s)$ and $\mathcal{O}(N_f^2\alpha^3, N_f^3\alpha^3)$ contributions beyond the leading m_t^4 and m_t^6 terms, respectively. (Here N_f^n denotes diagrams with n closed fermion loops. Based on experience from lower orders, the $\mathcal{O}(\alpha^3)$ diagrams with several closed fermion loops are expected to be dominant.) The calculation of these corrections requires three-loop vertex integrals with self-energy sub-loops and general three-loop self-energy integrals, which realisitically can be expected to be worked out in the forseeable future. The remaining $\mathcal{O}(\alpha^3)$ and four-loop terms should amount to $\sim10^{-5}$.[2]

When extracting $\sin^2\theta^\ell_{\rm eff}$ from $A_{\rm FB}$ and $A_{\rm LR}$, the initial- and final-state QED radiator functions $\mathcal{R}_i$ must be taken into account. In general, the QED corrections are known to $\mathcal{O}(\alpha)$ for the differential cross section and to $\mathcal{O}(\alpha^2)$ for the integrated cross section (see Ref. [63] for a summary). However, for the LR asymmetry they complete cancel up to NNLO [64], while for the FB asymmetry they cancel if hard photon contributions are excluded, i.e. they cancel up to terms of order $E_\gamma/\sqrt{s}$ [64, 65, 66]. Therefore, a sufficiently precise result for the soft-photon contribution with $E_\gamma < E_\gamma^{\rm cut}$ can be obtained using existing calcations for small enough $E_\gamma^{\rm cut}$, while the hard-photon contribution ($E_\gamma > E_\gamma^{\rm cut}$) can be evaluated with numerical Monte-Carlo methods.

Other important Z pole observables are R_b and the Z width. For the branching fraction $R_b = \Gamma_b/\Gamma_{\rm had}$, two-loop corrections of $\mathcal{O}(\alpha\alpha_s)$, $\mathcal{O}(N_f\alpha^2)$, and $\mathcal{O}(N_f^2\alpha^2)$ are known [67, 68]. Assuming geometric progression of the perturbative series, the remaining higher-order contributions are estimated to contribute at the level of $\sim 2\times10^{-4}$. As before, the contribution from electroweak two-loop diagrams without closed fermion loops is expected to be small. The dominant missing contributions are the same as for $\sin^2\theta^q_{\rm eff}$.

For the total width Γ_Z, only an approximate result for the electroweak two-loop corrections in the limit of large m_t is known [69]. The remaining $\mathcal{O}(N_f\alpha^2)$ may be relatively large, as turned out to be the case for R_b [68]. Based on the result for R_b, the uncertainty on Γ_Z associated with these corrections is estimated to be a few MeV, which is by far dominant compared to missing three-loop contributions. However, the $\mathcal{O}(N_f\alpha^2)$ correction can be computed with existing methods without conceptual difficulties.

Besides Z-pole observables, the W-boson mass, M_W plays an important role for electroweak precision physics. Theoretically, it can be predicted from the muon decay rate. After subtraction of QED radiation effects [70], muon decay can be described by an effective four-fermion interaction with the Fermi coupling constant G_μ, which in the SM is given by

$$\frac{G_\mu}{\sqrt{2}} = \frac{\pi\alpha M_Z^2}{2M_W^2(M_Z^2-M_W^2)}(1+\Delta r), \tag{1.8}$$

where Δr summarizes the electroweak (non-QED) higher-order corrections. This equation can be solved numerically for M_W.

Within the SM, M_W has been computed including full two-loop corrections [71, 72] and leading 3- and 4-loop corrections [58, 59, 60]. The intrinsic theoretical error is estimated to be about 4 MeV, mostly due from missing $\mathcal{O}(\alpha^2\alpha_s)$ and $\mathcal{O}(N_f^2\alpha^3, N_f^3\alpha^3)$ contributions beyond the leading-m_t approximation. Inclusion of these effects, which would require the computation of the 3-loop self-energies, would reduce the perturbative error to less than 1 MeV.

[2] This estimate can be made more precise only after aforementioned calculations have been completed.

Quantity	Current theory error	Leading missing terms	Est. future theory error
$\sin^2\theta^\ell_{\rm eff}$	4.5×10^{-5}	$\mathcal{O}(\alpha^2\alpha_s)$, $\mathcal{O}(N_f^{\geq2}\alpha^3)$	$1...1.5\times10^{-5}$
R_b	$\sim2\times10^{-4}$	$\mathcal{O}(\alpha^2)$, $\mathcal{O}(N_f^{\geq2}\alpha^3)$	$\sim1\times10^{-4}$
Γ_Z	few MeV	$\mathcal{O}(\alpha^2)$, $\mathcal{O}(N_f^{\geq2}\alpha^3)$	<1 MeV
M_W	4 MeV	$\mathcal{O}(\alpha^2\alpha_s)$, $\mathcal{O}(N_f^{\geq2}\alpha^3)$	$\lesssim1$ MeV

Table 1-1. *Some of the most important precision observables for Z-boson production and decay and the W mass (first column), their present-day estimated theory error (second column), the dominant missing higher-order corrections (third column), and the estimated improvement when these corrections are available (fourth column). In many cases, the leading parts in a large-mass expansion are already known, in which case the third column refers to the remaining pieces at the given order. The numbers in the last column are rough order-of-magnitude guesses.*

	$\Delta m_t=0.9$ GeV	$\Delta(\Delta\alpha_{\rm had})=1.38(1.0)\cdot10^{-4}$	$\Delta M_Z=2.1$ MeV	missing h.o.	total
ΔM_W [MeV]	5.4	2.5(1.8)	2.6	4.0	7.6(7.4)
$\Delta\sin^2\theta^\ell_{\rm eff}[10^{-5}]$	2.8	4.8(3.5)	1.5	4.5	7.3(6.5)

Table 1-2. *Current parametric and theory uncertainties of SM predictions of M_W and $\sin^2\theta^\ell_{\rm eff}$.*

The current status of the theoretical calculations and prospects for the near future are summarized in Tab. 1-1. Note that $\sigma_{\rm non-res}$ in eq. 1.2 is suppressed by Γ_Z/M_Z compared to the leading pole term, so that the known one-loop corrections are sufficient to reach NNLO precision at the Z pole.

The known corrections to the effective weak mixing angles and the partial widths are implemented in programs such as `Zfitter` [63, 73] and `Gfitter` [74]. However, these programs are based on a framework designed for NLO but not NNLO corrections. In particular, there are mismatches between the electroweak NNLO corrections to the $Zf\bar{f}$ vertices and QED/QCD corrections to the external legs due to approximations and factorization assumptions. Another problem is the separation of leading and sub-leading pole terms in eq. 1.2 [57]. While these discrepancies may be numerically small, it would be desireable to construct a new framework that treats the radiative corrections to Z-pole physics systematically and consistently at the NNLO level and beyond. Such a framework can be established based on the pole scheme [75], where the amplitude is expanded about the complex pole $s=M_Z^2-iM_Z\Gamma_Z$, with the power counting $\Gamma_Z/M_Z\sim\alpha$.

In addition to intrinsic theoretical error, the predictions of $\sin^2\theta^\ell_{\rm eff}$, M_W, *etc.* also depend on input parameters and their experimental uncertainties. The parametric uncertainties in the currently best SM predictions for M_W and $\sin^2\theta^l_{\rm eff}$ of Tables 1-2,1-3 have been determined with the help of the parametrization formulae of Ref. [72] for M_W and of Ref. [57] for $\sin^2\theta^\ell_{\rm eff}$.

Two recent determinations of the five-quark hadronic contribution to $\alpha(M_Z)$ find $\Delta\alpha^{(5)}_{\rm had}(M_Z)=(275.7\pm1.0)\cdot10^{-4}$ [76] and $\Delta\alpha^{(5)}_{\rm had}(M_Z)=(276.26\pm1.38)\cdot10^{-4}$ [77]. The residual theory uncertainties due to missing higher order corrections as listed in Table 1-2 have been taken from Refs. [72, 57]. Using the following measured values in the calculation of M_W and $\sin^2\theta^l_{\rm eff}$: $m_t=173.2\pm0.9$ GeV [78], $\alpha_s(M_Z)=0.1184\pm0.0007$ [79], $M_Z=91.1876\pm0.0021$ GeV [53], and $M_H=125\pm1$ GeV, one finds $M_W=80.3603\pm0.0076$ GeV and $\sin^2\theta^l_{\rm eff}=0.23127\pm0.00007$ for $\Delta\alpha_{\rm had}(M_Z)=(276.26\pm1.38)\times10^{-4}$ [77] and $M_W=80.3614\pm0.0074$ GeV and $\sin^2\theta^l_{\rm eff}=0.23129\pm0.00007$ for $\Delta\alpha_{\rm had}(M_Z)=(275.7\pm1.0)\cdot10^{-4}$ [76].

	$\Delta m_t = 0.6(0.1)$ GeV	$\Delta(\Delta\alpha_{\rm had}) = 5 \times 10^{-5}$	$\Delta M_Z = 2.1$ MeV	missing h.o.	total
ΔM_W [MeV]	3.6(0.6)	1.0	2.6	1.0	4.7(3.0)
$\Delta \sin^2\theta^\ell_{\rm eff}[10^{-5}]$	1.9(0.3)	1.8	1.5	1.0	3.2(2.6)

Table 1-3. *Anticipated parametric and theory uncertainties of SM predictions.*

In many new physics models, the leading contributions beyond the SM to electroweak precision observables can be described by the *oblique* parameters S, T, U [80]:

$$\Delta r \approx \Delta r^{\rm SM} + \frac{\alpha}{2s_W^2}\Delta S - \frac{\alpha c_W^2}{s_W^2}\Delta T + \frac{s_W^2 - c_W^2}{4s_W^4}\Delta U, \tag{1.9}$$

$$\sin^2\theta^\ell_{\rm eff} \approx (\sin^2\theta^\ell_{\rm eff})^{\rm SM} + \frac{\alpha}{4(c_W^2 - s_W^2)}\Delta S - \frac{\alpha s_W^2 c_W^2}{c_W^2 - s_W^2}\Delta T, \tag{1.10}$$

where $s_W^2 = 1 - c_W^2 = 1 - M_W^2/M_Z^2$, and S, T, U are given at 1-loop level in terms of the transverse parts of 1-PI gauge boson self-energies, $\Pi_{VV'}$:

$$\alpha S = 4s_W^2 c_W^2 \left[\Pi'_{ZZ}(0) - \frac{c_W^2 - s_W^2}{s_W c_W}\Pi'_{Z\gamma} - \Pi'_{\gamma\gamma}(0)\right], \tag{1.11}$$

$$\alpha T = \Delta\rho = \frac{\Pi_{WW}(0)}{M_W^2} - \frac{\Pi_{ZZ}(0)}{M_Z^2}, \tag{1.12}$$

$$\alpha U = 4s_W^2 \left[\Pi'_{WW}(0) - c_W^2\Pi'_{ZZ}(0) - 2s_W c_W \Pi'_{Z\gamma} - s_W^2\Pi'_{\gamma\gamma}(0)\right]. \tag{1.13}$$

Note that $\Delta T = 0$ ($\delta\rho = 0$) and $\Delta U = 0$ in case of exact custodial $SU(2)$ symmetry.

1.2.2 Uncertainties in measurements of M_W and $\sin^2\theta^l_{\rm eff}$ at hadron colliders

1.2.2.1 Theory and PDF aspects: M_W

Authors: Alessandro, Juan, Doreen

In hadronic collisions, the W boson mass can be determined from the transverse mass distribution of the lepton pair, $M_T(l\nu)$, originating from the W decay, $W \to \ell\nu$, and the transverse momentum distribution of the charged lepton or neutrino. Both QCD and electroweak (EW) corrections play an important role in the measurement of W boson observables at hadron colliders. For the anticipated experimental precision in the measurement of M_W at the Tevatron and the LHC, as presented in Section 1.2.2.2, it is imperative to control predictions for the relevant observables at the per mile level. For instance, the transverse momentum distribution of the W boson is an important ingredient in the current W mass measurement at the Tevatron (see, e.g. Ref. [167] for a review). In lowest order (LO) in perturbation theory, the W boson is produced without any transverse momentum. Only when QCD corrections are taken into account does the W boson acquire a non-negligible transverse momentum, p_T^W. For a detailed understanding of the p_T^W distribution, it is necessary to resum the soft gluon emission terms, and to model non-perturbative QCD corrections. This has either be done using calculations targeted specifically for resummation and parametrizing non-perturbative effects (see e.g. Refs. [168] and [169]), or interfacing a calculation of W boson production at next-to-leading order (NLO) in QCD with a parton-shower Monte Carlo (MC) program and tuning the parameters used to describe the non-perturbative effects. This approach has been pursued in Refs. [170, 171, 172]. Fixed

higher-order QCD corrections to fully differential distributions in W production are known through next-to-next-to-leading order [173, 174, 175].

While QCD corrections only indirectly affect the W mass extracted from the $M_T(l\nu)$ distribution, EW radiative corrections can considerably distort the shape of this distribution in the region sensitive to the W mass. For instance, final-state photon radiation is known to shift M_W by $\mathcal{O}(100$ MeV) [**?**, **?**, 176, 177, 178, 179, 180, 181]. In the last few years, significant progress in providing predictions including EW corrections to W boson production in hadronic collisions has been made. The complete $\mathcal{O}(\alpha)$ EW radiative corrections to $p\overset{(-)}{p} \to W^{\pm} \to \ell^{\pm}\nu$ ($\ell = e,\ \mu$) were calculated by several groups [182, 183, 184, 185, 186, 187, 188] and found to agree [189, 190]. First steps towards going beyond fixed order in QED radiative corrections in W production were taken in Refs. [191, 192, 193, 194, 195] by including the effects of final-state multiple photon radiation. For a review of the state-of-the-art of predictions for W and Z boson production at hadron colliders see, e. g., Refs. [189, 190, 196]. Given the anticipated accuracy of a W boson mass measurement at the Tevatron and the LHC, it is necessary to not only fully understand and control separately higher-order QCD and EW corrections, but also their combined effects. A first study of combined effects can be found in Ref. [197], where final-state photon radiation was added to a calculation of W boson production which includes NLO and resummed QCD corrections. This study showed that the difference in the effects of EW corrections in the presence of QCD corrections and of simply adding the two predictions may be not negligible in view of the anticipated precision. Moreover, in the relevant kinematic region, i.e. around the Jacobean peak, the QCD correction tend to compensate some of the effects of the EW corrections. In Ref. [198] the full set of EW $\mathcal{O}(\alpha)$ corrections of `HORACE` [187] and the QCD NLO corrections to W production were combined in the `MC@NLO` framework [170] which is interfaced with the parton-shower MC program `Herwig` [199]. The results of a combination of the EW $\mathcal{O}(\alpha)$ corrections to W and Z production as implemented in `SANC` [186, 200] with `Pythia` [201] and `Herwig` can be found in Ref. [202], without, however, performing a matching of NLO QCD corrections to the parton shower. Recently, the complete EW $\mathcal{O}(\alpha)$ radiative corrections to W and Z boson production became available in `POWHEG` [206, 207, 208], which allows to study the effects of NLO EW corrections in the presence of QCD radiation and with both `Pythia` and `Herwig`. However, this approach can only capture part of the two-loop mixed QCD-EW corrections, and only a complete 2-loop calculation of $\mathcal{O}(\alpha\alpha_s)$ corrections will provide a reliable estimate of the theoretical uncertainty due to missing higher-order corrections. In view of recent improvements in the calculation of two-loop corrections [**?**], it is reasonable to expect that these calculations are available at the timescale of a final LHC measurement of M_W.

Apart from providing precise predictions for W boson observables, also the PDF uncertainty has to be considerably reduced for a target uncertainty of $\Delta M_W = 9(5)$ MeV at the Tevatron(LHC), which is discussed in detail in Section 1.2.2.2.

1.2.2.2 Experimental aspects: M_W

Authors: Ashutosh

The Tevatron experiments have made precise measurements of the W boson mass. The combined uncertainty on M_W using CDF and DO measurements is 16 MeV, significantly surpassing the combined LEP precision of 33 MeV. This is a noteworthy achievement for hadron collider experiments. Furthermore, additional statistics are available at the Tevatron (approximately a factor of 4 at CDF and a factor of 2 at DO) and very large samples are available at the LHC (which will grow further in the coming years). The Tevatron experiments have demonstrated that many systematic uncertainties related to calibrations can be reduced as the statistics of the calibration samples and other control samples increase. This is a non-trivial demonstration since consistency between multiple calibration methods and channels is an essential component of a robust analysis.

ΔM_W [MeV]	CDF	D0	combined	final CDF	final D0	combined
$\mathcal{L}[\text{fb}^{-1}]$	2.2	4.3(+1.1)	7.6	10	10	20
PDF	10	11	10	5	5	5
QED rad.	4	7	4	4	3	3
$p_T(W)$ model	5	2	2	2	2	2
other systematics	10	18	9	4	11	4
W statistics	12	13	9	6	8	5
Total	19	26(23)	16	10	15	9

Table 1-4. *Current and projected uncertainties in the measurement of M_W at the Tevatron.*

Uncertainties due to parton distribution functions (PDFs) and electroweak radiative corrections rely on external experimental and theoretical input. Improvements in theoretical calculations have led to reductions in the latter. Collider measurements of boson distribtions have provided constraints on PDFs and increased statistics in the future should continue to do so.

Table 1-4 shows the projections from CDF and DO on the M_W uncertainty they expect to achieve with their respective final datasets from the Tevatron. These projections build mostly on the 4-5 measurements that these experiments have each made over the last two decades, which show that careful analysis of data has led to the approximate scaling of many systematic uncertainties with statistics. The datasets have grown by a factor of 200-500 over this time period. The projections to the full dataset assume some improvement in the understanding of the tracking and calorimetry, modest improvement in the understanding of radiative corrections, and a factor of two improvement in the PDF uncertainty over the next few years. The analysis in Ref. [209] has shown that the LHC measurements of the W charge asymmetry using the 2012 data has the potential to reduce the W mass uncertainty at the Tevatron by about a factor of two. Thus, it is reasonable to assume that the final Tevatron measurements will achieve a combined uncertainty of 9-10 MeV, as projected.

According to Ref. [209], the PDF uncertainty at the LHC is about a factor of two larger than at the Tevatron. Thus, further improvements in the PDF uncertainty will be required to produce higher precision on the W boson mass. This will require a program of measurements of differential boson distributions such as (i) the Z boson rapidity distribution, (ii) the charged lepton rapidity distribution from W boson decays, (iii) the W charge asymmetry distribution, and (iv) the W+charm production which constrains the strange quark contribution. Combined with the increasing understanding of the LHC detectors, we suggest that a PDF uncertainty below 5 MeV is a reasonable target for the LHC (see also Sec. 1.2.2.1 for a detailed discussion). As shown in Table 1-5, we propose targets for m_W precision at the LHC, approaching 5 MeV in the long term. Note that detailed detector studies and improved analysis techniques are just as important in this endeavor as the growth of the data statistics. We consider having a 5 MeV target for the total precision as a reasonable ambition for the LHC.

1.2.2.3 Experimental aspects: $\sin^2\theta^l_{\text{eff}}$

Authors:
LHC discussion: Ashutosh, Regina Caputo
Tevatron discussion: Arie Bodek, Jiyeyon Han, Willis Sakumoto

Investigations around the Z resonance in single neutral-current vector-boson, $q\bar{q} \to \gamma, Z \to l^+l^-$, with charged leptons l in the final state, allow a precise measurement of the electroweak mixing angle from the

ΔM_W [MeV]	LHC		
$\sqrt{s}$ [TeV]	8	14	14
$\mathcal{L}[\text{fb}^{-1}]$	20	300	3000
PDF	10	5	3
QED rad.	4	3	2
$p_T(W)$ model	2	1	1
other systematics	10	5	3
W statistics	1	0.2	0
Total	15	8	5

Table 1-5. *Current and target uncertainties in the measurement of M_W at the LHC.*

forward-backward asymmetry A_{FB} at hadron colliders. The results of a measurement of $\sin^2\theta^l_{eff}$ at the Tevatron by the CDF and D0 collaborations and at the LHC by the ATLAS and CMS collaborations are presented in Table 1-6 and Table 1-7, respectively.

At the Tevatron, because the quark direction is better defined for $\bar{p}p$ than for pp collisions, the measurement of $\sin^2\theta^l_{\text{eff}}$ is less sensitive to PDF uncertainties and higher order QCD corrections. In addition, three significant improvements have been recently introduced in the analysis at CDF. The first is the introduction of the event weighting technique[81], which to first order results in the cancellation of acceptance errors and also reduces the statistical errors by 20%. The second is the introduction of momentum scale corrections[82], which remove the bias in the determination of muon momenta, and the third is the consideration of electroweak radiative corrections using Zfitter[49]. Therefore, smaller error bars are expected for the final analysis of the full Run II Tevatron data as shown in Table 1-6. The errors in the e^+e^- channel are smaller than in the $\mu^+\mu^-$ channel, if forward electrons (i.e. large $\cos\theta$) are included in the analysis. Based on the recent improvements in the CDF analysis, we expect similar errors with the full Run II data set at D0.

In addition to the determination of $\sin^2\theta^l_{\text{eff}}$, a measurement of A_{FB} in the Z boson region can also be used to extract the Standard Model (SM) value of $\sin^2\theta_W = 1 - M_W^2/M_Z^2$[49] and thus an *indirect* determination of M_W^{OS} defined within the SM in the on-shell (OS) renormalization scheme. For example, the recent CDF measurement[49] with an e^+e^- sample corresponding to 2.1 fb^{-1} of integrated luminosity yields (statistical and systematic errors are added linearly): $\sin^2\theta^l_{\text{eff}} = 0.2328 \pm 0.0011$, $\sin^2\theta_w = 0.2246 \pm 0.0011$, and $M_W(indirect)^{OS} = 80.297 \pm 0.055\ GeV$. For comparison, the *indirect* prediction of M_W^{OS} within the SM from a global fit to Z pole LEP/SLC data yields $M_W^{OS} = 80.359 \pm 0.011$ GeV [84], and the global fit to all data (excluding the direct M_W measurement) yields $M_W^{OS} = 80.360 \pm 0.008$ GeV. Comparing *direct* measurements with *indirect* determinations of SM input parameters provides a powerful consistency check of the underlying theory.

At the LHC, the measurement of the forward-backward asymmetry A_{FB} at the Z boson pole is complicated by the fact that the pp initial state dilutes the A_{FB} in the $q\bar{q}$ collision. As a result, the measurement is sensitive to the PDFs. Table 1-7 shows the uncertainties from the current LHC analyses. Systematic uncertainties due to experimental effects will very likely reduce with higher statistics as efficiencies and resolutions are better measured using control samples. In order to exploit this potential, however, a significant improvement in the understanding of PDFs will be required. We note that the PDF uncertainty will need to reduce by a factor of ~ 7 for the LHC measurement of $\sin^2\theta^l_{\text{eff}}$ to have comparable precision as the LEP and SLC measurements. A factor of 2 reduction in the systematic uncertainty due to missing higher order corrections will also be required. In the following we discuss in more detail the challenges involved in reaching the target uncertainties shown in Table 1-7 based on the experience from the recent ATLAS analysis.

$\Delta \sin^2\theta^l_{\rm eff}$ $[10^{-5}]$	CDF	D0	final CDF	final CDF	final CDF
final state	e^+e^-	e^+e^-	$\mu^+\mu^-$	e^+e^-	combined
$\mathcal{L}[\,\mathrm{fb}^{-1}]$	2.1	5.0	9.0	9.0	9.0 $\mu\mu + 9$ e^+e^-
PDF	12	48	12	12	12
higher order corr.	13	8	13	13	13
other systematics	5	38	5	5	5
statistical	90	80	80	40	40
total $\Delta \sin^2\theta^l_{\rm eff}$	**92**	**101**	**82**	**44**	**41**

Table 1-6. *Current and target uncertainties in the measurement of* $\sin^2\theta^l_{\rm eff}$ *at the Tevatron.*

$\Delta \sin^2\theta^l_{\rm eff}$ $[10^{-5}]$	ATLAS	CMS	LHC/per experiment		
$\sqrt{s}$ [TeV]	7	7	8	14	14
$\mathcal{L}[\,\mathrm{fb}^{-1}]$	4.8	1.1	20	300	3000
PDF	70	130	35	25	10
higher order corr.	20	110	20	15	10
other systematics	70	181	60(35)	20	15
statistical	40	200	20	5	2
Total	108	319	75(57)	36	21

Table 1-7. *Current and target uncertainties in the measurement of* $\sin^2\theta^l_{\rm eff}$ *at the LHC. The target uncertainties are based on expected advancements in both theory and experiment as described in the text. A conservative and more optimistic (in parentheses) target uncertainty is provided for the measurement at 8 TeV.*

The main difficulty in measuring $\sin^2\theta^l_{\rm eff}$ at the LHC from the forward backward asymmetry, A_{FB}, lies in the fact that it is a pp collider. Since both beams have valence quarks (as opposed to anti-quarks), there is an ambiguity in the incoming quark direction. This ambiguity gives rise to a dilution, or reduction, in the A_{FB}. The effect of dilution can be resolved in part by using the momentum of the Z along the longitudinal direction (z) to determine the direction of the outgoing lepton with respect to the quark. However, for events produced in the central part of the detector, there remains about a 50% probability of misidentifying the quark direction. Therefore the best region of phase space to make this measurement is at large Z p_z, or equivalently rapidity.

The ATLAS $\sin^2\theta^l_{\rm eff}$ measurement utilizes electrons and muons not only in the central region of the detector, which are standard for most measurements, but also electrons in the forward region ($2.5< |\eta| <4.9$). However, there are some difficulties in using forward electrons. Mainly the forward calorimeters are not as highly segmented and there are no tracking detectors, so reconstruction relies on less information. Also, distinguishing between photons and electrons is not possible. Finally, electrons in the forward region are more sensitive to pile-up, which not only increases the background but also makes background modeling more difficult. These difficulties can be overcome by requiring one central electron and one forward electron in the Z reconstruction.

This approach means that ATLAS has produced three search channels in total in the 2011 analysis: a muon channel with two central muons, an electron channel with two central electrons (CC electron), and an electron channel with one central electron and one forward electron (CF channel). To measure $\sin^2\theta^l_{\rm eff}$,

the A_{FB} spectra from data were compared to the asymmetry spectra from Monte Carlo (MC) predictions produced with varying initial values of the weak mixing angle. The results from the three channels are as follows

$$\text{CC electron} : \sin^2\theta^l_{\text{eff}} = 0.2288 \pm 0.0009(\text{stat.}) \pm 0.0014(\text{syst.})$$

$$\text{muon} : \sin^2\theta^l_{\text{eff}} = 0.2294 \pm 0.0009(\text{stat.}) \pm 0.0014(\text{syst.})$$

$$\text{CF electron} : \sin^2\theta^l_{\text{eff}} = 0.2304 \pm 0.0006(\text{stat.}) \pm 0.0010(\text{syst.})$$

Despite having fewer events, the CF electron has the smallest total uncertainty. This is due to the reduced effect of dilution in this channel, which allows better discrimination between the MC templates. The uncertainties in the combined ATLAS measurement of $\sin^2\theta^l_{\text{eff}} = 0.2297 \pm 0.0004(\text{stat.}) \pm 0.009(\text{syst.})$ are outlined in Table 1-7. The systematic uncertainty is dominated by the PDF uncertainty (0.0007) which is correlated and therefore did not see the reduction that the other uncertainties did. This uncertainty was estimated using the CT10 NLO PDF set. The total uncertainty for this measurement matches the precision of the most recent results from the Tevatron experiments shown in Table 1-6.

The $\sin^2\theta^l_{\text{eff}}$ ATLAS measurement is limited by the PDF uncertainty in the two central channels, and by the energy scale and smearing in the CF electron channel [52]. The future of this measurement lies in reducing the PDF uncertainty for the central channels. It is a factor of 2 larger than the next largest uncertainty. However, it is the CF electron channel that shows the most potential for being competitive with the LEP and SLC experiments. If the PDF and energy scale/smearing uncertainties were both reduced by a factor of two, ATLAS would become competitive. Although the energy scale/smearing will be increasingly difficult with increased pile-up conditions as well as higher trigger thresholds due to the increased luminosity, the increased statistics as well as better knowledge of the detector (with more use and simulation) will allow us to work toward a significant reduction.

For the 2012 projection with 8 TeV and 20 fb^{-1} of data shown in Table 1-7, the PDF and energy scale/smearing uncertainties will most likely not be reduced to the point where it will be competitive with the world's best measurements. The statistical uncertainty will be reduced by a factor of two (with the 4x increase in data). The MC statistical uncertainty can be reduced to a negligible amount which reduces the "other systematics" column to 6 instead of 7 in a conservative scenario (shown in parentheses is a more optimistic scenario where it is assumed that energy scale/smearing uncertainties can be considerably reduced). Assuming that the inclusion of LHC data in updated PDF fits yields a reduction of the PDF error by a factor of 2 (see discussion in Section 1.2.2.1), this would lead to a total uncertainty of $75(57)\times10^{-5}$.

The target uncertainties for a future ATLAS measurement of $\Delta\sin^2\theta^l_{\text{eff}}$ shown in Table 1-7 are based on the following reasoning and expectations for advancements in both theory and experiment. We assume that with advancements in MC generators the uncertainty due to higher order corrections will decrease dramatically. Currently this is taken as a systematic uncertainty in the ATLAS and CMS measurements, however in the future, it could just be a shift or not required at all. It is very difficult to reduce the energy scale/smearing uncertainty in the forward channel. However, up until now there was no motivation to do so, since the PDF uncertainty was the limiting factor. It is reasonable to expect that one could push the bounds on the energy scales/smearing, if this became the limiting systematic. The last challenge will be triggering on CF electron events. Since there is only one central electron, we rely on the single electron trigger. For the 2015 run, these thresholds will increase dramatically from the 2012 level making it harder to trigger on Standard Model events. There is currently work going on to overcome this challenge, so that forward electron Z events can still be used in the future.

1.2.3 Uncertainties in measurements of M_W and $\sin^2\theta^l_{\mathbf{eff}}$ at lepton clolliders

1.2.3.1 Theory status of W-pair production at e^+e^- colliders

Author: C.Schwinn

The possibilities offered by future e^+e^- colliders make it mandatory to improve the accuracy of the theoretical predictions of the $e^+e^- \to W^+W^-$ cross section beyond the level achieved for LEP2. A precise measurement of m_W with an accuracy $\sim$ 5MeV from a threshold scan in the GigaZ option of an ILC or at TLEP requires a cross-section calculation with a precision of a few per-mille in the threshold region $\sqrt{s} \sim 2m_W$. At high center of mass energies $\sqrt{s} \gtrsim 800$ GeV in the second phase of an ILC or at CLIC, which are particularly relevant for measurements of anomalous triple gauge couplings, electroweak radiative corrections are enhanced so that NNLO corrections can become relevant. In the following we review recent calculations that improve the theoretical predictions in these regimes and assess the remaining theoretical uncertainties.

Precise theoretical predictions for W-pair production have to take the W-boson decay into account and treat the full 4-fermion final state. The state of the art during the LEP2 run consisted of the so-called double-pole approximation (DPA) utilized in the computer programs RACOONWW [157] and YFSWW3 [158]. In the DPA the quantum corrections to four-fermion production are consistently decomposed into the corrections to on-shell W-boson production and decay (factorizable corrections), soft-photon corrections connecting W-production, propagation and decay stages (non-factorizable corrections), and into a non-resonant remainder. More recently, a complete NLO calculation of 4-fermion production was performed [159], including loop corrections to singly- and non-resonant diagrams and treating unstable particles in the complex mass scheme. As can be seen in Figure 1-1 the results of the DPA for the total cross section agree well with the full $e^+e^- \to$ 4f calculation for energies $200\,\text{GeV} \lesssim \sqrt{s} \lesssim 500\,\text{GeV}$ while the full calculation is required in the threshold region $160\,\text{GeV} \lesssim \sqrt{s} \lesssim 170\,\text{GeV}$ and at energies $s > 500\,\text{GeV}$ where off-shell effects become important. The description of differential distributions for hadronic W-decays could be improved in the future since presently only QCD corrections to the inclusive W-decay width are included.

At center of mass energies $s \gg m_W^2$ as relevant for the measurement of anomalous triple gauge boson couplings, large radiative corrections to W-pair production arise due to so-called Sudakov logarithms $\log^2(s/m_W^2)$ [160]. The NNLO corrections to on-shell W-pair production at NNLL accuracy (*i.e.* corrections of the form $\alpha^2 \log^m(s/m_W^2)$ with $m = 2, 3, 4$) have been computed in [161]. They are of the order of 5% (15%) for $\sqrt{s} = 1\,\text{TeV}$ ($\sqrt{s} = 3\,\text{TeV}$) and therefore should be taken into account in the second phase of an ILC or at CLIC. The remaining uncertainty due to the uncalculated single-logarithmic NNLO terms has been estimated to be 1–2% [161]. It might also be relevant to consider NNLO Sudakov logarithms for the full 4-fermion final state instead of using the approximation of on-shell W-bosons.

Near the W-pair production threshold, Coulomb corrections of the form $(\alpha/\beta)^n$, with $\beta = \sqrt{1 - 4m_W^2/s}$, are enhanced over the remaining corrections of the same order in α. Therefore the second-order Coulomb correction $\sim (\alpha/\beta)^2$ [162] and contributions of the form α^2/β are expected to be the dominant NNLO corrections near threshold and have been calculated in [163] using an effective-field theory (EFT) approach [164]. As can be seen in Figure 1-2, the effect of the threshold-enhanced NNLO corrections is of the order of 0.5%. The remaining uncertainty of the m_W-measurement from a threshold scan due to uncalculated NNLO corrections has been estimated to be below $\Delta m_W \approx$ 3MeV [163]. The current best prediction for the total cross section near threshold is obtained by adding the dominant NNLO corrections to the NLO_{ee4f} result [159] that includes one-loop singly and non-resonant diagrams beyond the NLO EFT calculation. For the future, a calculation of the leading NNLO corrections for differential distributions is desirable. As a caveat, further uncertainties arise since the cross section at threshold is very sensitive to initial-state radiation (ISR). In the NLO_{EFT} and $\Delta\text{NNLO}_{\text{thresh}}$ results in Figure 1-2 as well as in the DPA and ee4f results in Figure 1-1,

a leading-logarithmic resummation of ISR effects [165] is performed for the Born cross section while higher-order corrections are added without ISR improvement. In the blue-dashed curve in Figure 1-2, instead also the higher-order EFT corrections are improved by ISR resummation.[3] The numerical impact of this next-to-leading logarithmic (NLL) effect is as large as 2% directly at threshold while it soon becomes negligible at higher energies. Therefore a consistent NLL-treatment of ISR might be required for sufficient theoretical control over the cross section at threshold.

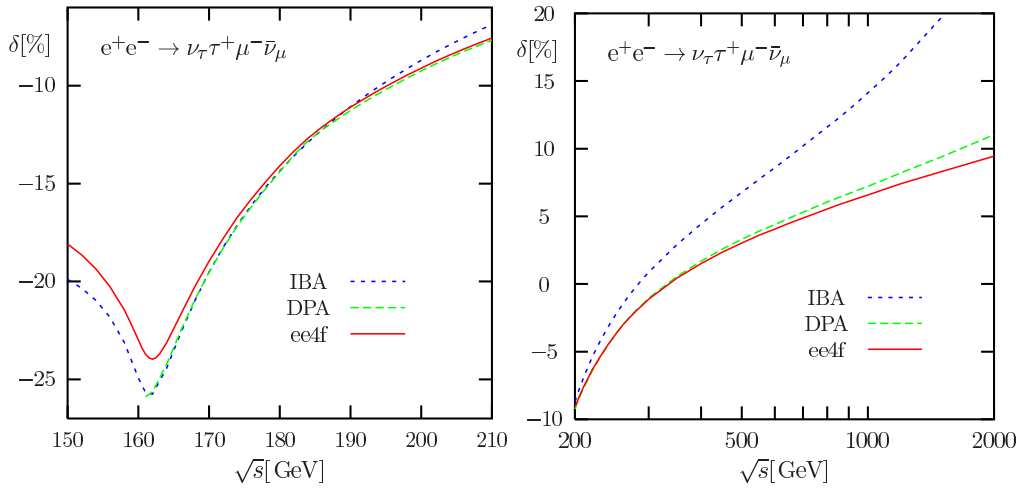

Figure 1-1. *Relative corrections to the total cross section for $e^+e^- \to \nu_\tau\tau^+\mu^-\bar{\nu}_\mu$, normalized by the Born cross section without ISR improvement: improved Born approximation (IBA, blue dashed), double-pole approximation (DPA, green short-dashed) and the NLO calculation for the 4-fermion final state (ee4f, red). Taken from Ref. [159].*

1.2.3.2 Experimental aspects: M_W

Authors: Graham Wilson

The three most promising approaches to measuring the W mass at an e^+e^- collider are:

- Polarized threshold scan of the W^+W^- cross-section as discussed in [139].
- Kinematically-constrained reconstruction of W^+W^- using constraints from four-momentum conservation and optionally mass-equality as was done at LEP2.
- Direct measurement of the hadronic mass. This can be applied particularly to single-W events decaying hadronically or to the hadronic system in semi-leptonic W^+W^- events.

The three different methods are summarized in the following tables. There is one reasonably complete study related to a polarized threshold scan at ILC [139] which has been updated for this Snowmass workshop. There is also a new much more precise method for determining the beam energy in situ using di-muon events at ILC which has been developed in more depth during this workshop and was presented at [140]. This gives the potential to reduce the beam energy uncertainty on the W mass to 0.8 MeV (limited by stand-alone momentum scale uncertainties estimated at 10 ppm). This previously important systematic for

[3] Note that the IBA approximation in Figure 1-1 also contains ISR improvement of the first Coulomb correction.

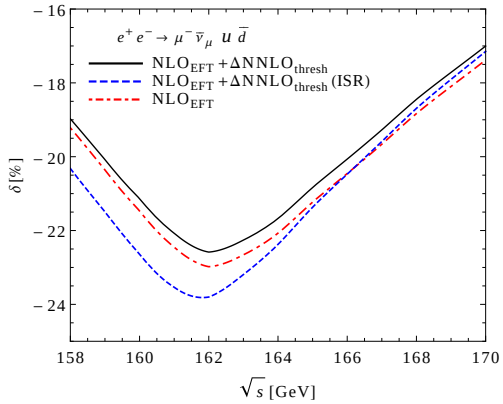

Figure 1-2. *Relative corrections to the total cross section for $e^+e^- \to \mu^-\bar{\nu}_\mu u\bar{d}$ in the EFT approach, normalized by the Born cross section without ISR improvement: NLO (red, dash-dotted), NLO with dominant NNLO corrections (black, solid). In the blue, dashed curve the higher-order corrections are convoluted with ISR structure functions. Based on Ref. [163].*

the threshold method - and dominant systematic for the kinematically-constrained reconstruction method appears to be no longer such a critical issue. The reported tables should be taken as reasonable indications of the potential performance. W mass measurements were statistics limited for these methods at LEP2. It is clear that large improvements in the systematics are feasible at future machines like ILC. Exactly how much better can be done is something that can not be predicted with absolute certainty, given the orders of magnitude of improvement. In practice it is something that typically can only be pinned down once a detector is operating. In general the experience has been that predictions tend to err significantly on being too conservative.

ΔM_W [MeV]	LEP2	ILC	ILC	LEP3	TLEP
$\sqrt{s}$ [GeV]	161	161	161	161	161
$\mathcal{L}$ [fb^{-1}]	0.040	100	480	600	3000
$P(e^-)$ [%]	0	90	90	0	0
$P(e^+)$ [%]	0	60	60	0	0
systematics	70			?	?
statistics	200			2.3?	1.0?
experimental total	210	3.9	1.9	>2.3	>1.0
beam energy	13	0.8	0.8	0.8	0.1-0.8
theory	-	1.0	1.0	1.0	1.0
total	210	4.1	2.3	>2.6	>1.5

Table 1-8. *Current and preliminary anticipated uncertainties in the measurement of M_W at e^+e^- colliders close to WW threshold.*

Table 1-8 has projected results for running close to WW threshold. ILC can collide highly longitudinally polarized electrons and positrons - this is particularly advantageous for a threshold scan. In the tables it is assumed that if ILC undertakes a dedicated scan near threshold that this would be done with the highest polarization levels achievable. The estimated uncertainties assume that the beam energy scale

can be established from collision data at the level of 1 part in 10^5 leading to a corresponding experimental uncertainty on M_W of 0.8 MeV. This has been shown to be statistically feasible using di-muon events provided that the momentum scale is determined to the same precision. This appears feasible using J/ψ events in Z decays. It was not feasible to use resonant depolarization near 80.5 GeV in the LEP ring for an even more precise beam energy measurement - this may be possible but needs to be convincingly demonstrated for a very big ring like TLEP. The ILC numbers are based on a detailed and updated study with realistic assumptions on detection efficiency, polarization determination, backgrounds, efficiency and normalization errors using a 6-point scan with four different beam helicity combinations. The ILC numbers include the (small) effects from beamstrahlung on the cross-section and take advantage of the 150 fb cross-section of multi-hadron production for determinining the beam polarizations from the data. The LEP3 and TLEP numbers are an initial estimate based on extrapolating from the ILC study and need to be refined particularly in regards to control of the background which is a minor issue for ILC as it is measured in place using the polarization. In addition, the table includes an indicative estimate of the anticipated theoretical uncertainty associated with interpreting cross-section measurements near threshold in terms of M_W of 1.0 MeV. A detailed assessment of the anticipated theoretical shape and normalization uncertainties on the cross-section behavior with center-of-mass energy and including the effects of realistic experimental acceptance for all the four-fermion final states would in principle be needed to report a firm theoretical error estimate. In the table for the ILC, the systematics are essentially currently included in the overall error as the multi-parameter fit adjusts the systematics as nuisance parameters constrained within a priori uncertainties taken as 0.1% for relative efficiency and absolute integrated luminosity. The beam polarizations and backgrounds are fitted simultaneously from the data. In the context of the polarized scan this measurement is essentially *statistics* dominated.

ΔM_W [MeV]	LEP2	ILC	ILC	ILC
$\sqrt{s}$ [GeV]	172-209	250	350	500
$\mathcal{L}$ [fb^{-1}]	3.0	500	350	1000
$P(e^-)$ [%]	0	80	80	80
$P(e^+)$ [%]	0	30	30	30
beam energy	9	0.8	1.1	1.6
luminosity spectrum	N/A	1.0	1.4	2.0
hadronization	13	1.3	1.3	1.3
radiative corrections	8	1.2	1.5	1.8
detector effects	10	1.0	1.0	1.0
other systematics	3	0.3	0.3	0.3
total systematics	21	2.4	2.9	3.5
statistical	30	1.5	2.1	1.8
total	36	2.8	3.6	3.9

Table 1-9. *Current and preliminary estimated experimental uncertainties in the measurement of M_W at e^+e^- colliders from kinematic reconstruction in the $q\bar{q}\ell\nu_\ell$ channel with $\ell = e, \mu$*

Table 1-9 has projected results for kinematic reconstruction using the semi-leptonic channels as was used at LEP2. Details of this method are in the recently submitted LEP2 legacy paper [141] and the systematics discussed there are used as the basis for this discussion. At LEP2 the fully hadronic channel was also used. It is not expected to be competitive at the sub-10 MeV level because of final-state interaction effects and is so is neglected for these projections. There have not been dedicated studies on the semi-leptonic channel for

ILC, but the measurements at LEP2 can be used to estimate/bracket some of the primary uncertainties. The beam energy uncertainty is taken again as a 10^{-5} uncertainty at 250 GeV leading to an error of 0.8 MeV. At higher energies this uncertainty is scaled linearly with center-of-mass energy reflecting in part less statistics for in-situ checks. Systematic errors associated with knowledge of the luminosity spectrum dL/dx_1dx_2 are estimated to be at the 1 MeV level at 250 GeV and will increase with center-of-mass energy. The table assumes a linear dependence. Two of the primary systematics associated with the W mass measurement at LEP2, namely from hadronization and detector effects will be controlled much better with the modern ILC detectors and a more than one hundred times larger data-set. In particular for example it is reasonable to expect that the 7 MeV error associated with a 0.3% uncertainty on the muon energy scale in for example the OPAL analysis is reduced to negligible (naively 0.02 MeV). The hadronization errors which dominated the LEP2 systematic uncertainty were a result of several effects. The much larger statistics envisaged at ILC will allow the kaon and proton fractions in W decays to be measured at least ten times better and the particle-flow based jet reconstruction should make it more feasible to use identified particles in reconstructing jets. Given the improvements in the detector and statistics, improvements in the leading experimental systematics by a factor of 10 can be envisaged. The radiative corrections systematic can presumably be improved with further work. The growing importance of ISR at higher center-of-mass energies suggests that this systematic will degrade as the center-of-mass energy increases. The effective statistical error is not completely straightforward to estimate as it includes effects from ISR and beamstrahlung which often degrade the validity of the kinematic constraints both of which are substantially larger at higher center-of-mass energy. It has been shown that these effects can be ameliorated in the fully hadronic channel [142] by allowing for such photon radiation. It is expected that similar methods will be useful to improve the effective resolution in the semi-leptonic channel too although this is not as highly constrained given the unobserved neutrino. This method is likely to be *systematics* dominated.

ΔM_W [MeV]	ILC	ILC	ILC	ILC
$\sqrt{s}$ [GeV]	250	350	500	1000
$\mathcal{L}$ [fb^{-1}]	500	350	1000	2000
$P(e^-)$ [%]	80	80	80	80
$P(e^+)$ [%]	30	30	30	30
jet energy scale	3.0	3.0	3.0	3.0
hadronization	1.5	1.5	1.5	1.5
pileup	0.5	0.7	1.0	2.0
total systematics	3.4	3.4	3.5	3.9
statistical	1.5	1.5	1.0	0.5
total	3.7	3.7	3.6	3.9

Table 1-10. *Preliminary estimated experimental uncertainties in the measurement of M_W at e^+e^- colliders from direct reconstruction of the hadronic mass in single-W and WW events where one W decays hadronically. Does not include WW with $q\bar{q}\ell\nu_\ell$ where $\ell = e, \mu$.*

Table 1-10 has projected results from the direct measurement of the hadronic mass. This measurement depends primarily on how well the hadronic mass scale can be determined. It essentially does not depend at all on measurements of the beam energy or luminosity spectrum and so is very complementary to the previous two methods. In the particle-flow approach it is in principle possible to cast this as primarily a "bottom-up" problem of determining the tracker momentum scale, the electro-magnetic calorimeter scale and the calorimeter energy scale for neutral hadrons and it is these components that affect the jet energy scale. Over the course of the envisaged ILC program it is anticipated that the samples of Z's decaying to hadrons

$\Delta \sin^2 \theta^l_{\text{eff}}$ $[10^{-5}]$	LEP/SLC	GigaZ	TLEP(Z)
systematics			
beam energy			
statistical			
theory			
Total	16	1	0.2

Table 1-11. *Current and target uncertainties in the measurement of* $\sin^2 \theta^l_{\text{eff}}$ *at lepton colliders.*

	LHC	LHC	GigaZ	ILC		TLEP(W)	SM prediction
$\sqrt{s}$ [TeV]	14	14	0.091	0.161	0.250	0.161	
$\mathcal{L}[\text{fb}^{-1}]$	300	3000		100(480)	500	3000	
ΔM_W [MeV]	8	5	-	4.1(2.3)	3.6	1.5	4.7(3.0)
$\Delta \sin^2 \theta_{\text{eff}}$ $[10^{-5}]$	36	21	1.0			0.2	3.2(2.6)

Table 1-12. *Experimental target accuracies at future hadron and lepton colliders and theory uncertainties of SM predictions. At present the measured and predicted values for* M_W *and* $\sin^2 \theta^l_{\text{eff}}$ *are:* $M_W^{exp} = 80.385 \pm 0.015$ *GeV*

where the Z mass is currently known to 2.1 MeV should make it feasible to target a 3.0 MeV error originating from the jet energy scale. The hadronization error is anticipated to be dominated by knowledge of the K^0_L and neutron fractions. The pile-up entry refers to primarily $\gamma\gamma \to$ hadrons events coincident with W events. The contribution of such events to the measured hadronic mass can be mitigated and is not expected to be a dominant systematic error - but it will be more problematic at higher center-of-mass energies. The statistical error depends on the jet energy resolution and the consequent hadronic mass resolution. The hadronic mass resolution for a particular event varies substantially depending primarily on the fractions of energy in charged particles, photons and neutral hadrons in the event. The effective hadronic mass resolution is therefore a strong function of the analysis method. A full convolution fit with more advanced reconstruction techniques like π^0 mass-constrained fitting offers the potential to improve the W mass statistical error by a factor of 2.2 over that naively estimated from the observed average jet energy resolution in full simulation studies. In the estimates below, we have been conservative and have assumed that the actual improvement factor of a realistic and mature analysis is 1.4. This method is likely to be *systematics* dominated.

1.2.3.3 Experimental aspects: $\sin^2 \theta^l_{\text{eff}}$

1.2.4 EWPO in the MSSM

Authors: Sven Heinemeyer, Georg Weiglein and Lisa Zeune

Precision measurements of SM observables have proven to be a powerful probe of BSM physics via virtual effects of the additional BSM particles. In general, precision observables (such as particle masses, mixing angles, asymmetries etc.) constitute a test of the model at the quantum-loop level, since they can be calculated within a certain model beyond leading order in perturbation theory, depending sensitively on the other model parameters, and can be measured with equally high precision. Various models predict different values of the same observable due to their different particle content and interactions. This permits

to distinguish between, e.g., the SM and a BSM model, via precision observables. Naturally, this requires a very high precision of both the experimental results and the theoretical predictions. (It should be kept in mind that the extraction of precision data often assumes the SM.) Important EWPOs are the W boson mass, M_W, and the effective leptonic weak mixing angle, $\sin^2\theta^\ell_{\rm eff}$, where the top quark mass plays a crucial role as input parameter. As an example for BSM physics the MSSM is a prominent showcase and will be used here for illustration.

The first analysis concerns the W boson mass. The prediction of M_W in the MSSM depends on the masses, mixing angles and couplings of all MSSM particles. Sfermions, charginos, neutralinos and the MSSM Higgs bosons enter already at one-loop level and can give substantial contributions to M_W. The evaluation used here consists of the complete available SM calculation, a full MSSM one-loop calculations and all available MSSM two-loop corrections [151, 143]. Due to the strong MSSM parameter dependences, it is expected to obtain restrictions on the MSSM parameter space in the comparison of the M_W prediction and the experimental value.

The results for the general MSSM can be obtained in an extensive parameter scan [143]. The ranges of the various SUSY parameters are given in Table 1-13. μ is the Higgsino mixing parameter, $M_{\tilde{F}_i}$ denotes the soft SUSY-breaking parameter for sfermions of the ith family for left-handed squarks ($F = Q$), right-handed up- and down-type squarks ($F = U, D$), left-handed sleptons ($F = L$) and right-handed sleptons ($F = E$). A_f denotes the trilinear sfermion-Higgs couplings, M_3 the gluino mass parameter and M_2 the SU(2) gaugino mass parameter, where the U(1) parameter is fixed as $M_1 = 5/3 s_w^2/c_w^2 M_2$. M_A is the CP-odd Higgs boson mass and $\tan\beta$ the ratio of the two Higgs vacuum expectation values.

Parameter	Minimum	Maximum
μ	-2000	2000
$M_{\tilde{E}_{1,2,3}} = M_{\tilde{L}_{1,2,3}}$	100	2000
$M_{\tilde{Q}_{1,2}} = M_{\tilde{U}_{1,2}} = M_{\tilde{D}_{1,2}}$	500	2000
$M_{\tilde{Q}_3}$	100	2000
$M_{\tilde{U}_3}$	100	2000
$M_{\tilde{D}_3}$	100	2000
$A_e = A_\mu = A_\tau$	-3 $M_{\tilde{E}}$	3 $M_{\tilde{E}}$
$A_u = A_d = A_c = A_s$	-3 $M_{\tilde{Q}_{12}}$	3 $M_{\tilde{Q}_{12}}$
A_b	-3 $\max(M_{\tilde{Q}_3}, M_{\tilde{D}_3})$	3 $\max(M_{\tilde{Q}_3}, M_{\tilde{D}_3})$
A_t	-3 $\max(M_{\tilde{Q}_3}, M_{\tilde{U}_3})$	3 $\max(M_{\tilde{Q}_3}, M_{\tilde{U}_3})$
$\tan\beta$	1	60
M_3	500	2000
M_A	90	1000
M_2	100	1000

Table 1-13. *MSSM parameter ranges. All parameters with mass dimension are given in GeV.*

All MSSM points included in the results have the neutralino as LSP and the sparticle masses pass the lower mass limits from direct searches at LEP. The Higgs and SUSY masses are calculated using `FeynHiggs` (version 2.9.4) [144, 145, 146, 147, 148]. For every point it was tested whether it is allowed by direct Higgs searches using the code `HiggsBounds` (version 3.8.0) [149, 150]. This code tests the MSSM points against the limits from LEP, Tevatron and the LHC.

The results for M_W are shown in Fig. 1-3 as a function of m_t, assuming the light CP-even Higgs h in the region $125.8 \pm 0.7(3.1)$GeV in the SM (MSSM) case. The red band indicates the overlap region of the SM and the MSSM. The leading one-loop SUSY contributions arise from the stop sbottom doublet. However requiring M_h in the region 125.8 ± 3.1GeV restricts the parameters in the stop sector [153] and with it the possible M_W contribution. Large M_W contributions from the other MSSM sectors are possible, if either charginos, neutralinos or sleptons are light.

The gray ellipse indicates the current experimental uncertainty, whereas the blue and red ellipses shows the anticipated future LHC and ILC/GigaZ precisions, respectively (for each collider experiment separately). While at the current level of precision SUSY might be considered as slightly favored over the SM by the M_W-m_t measurement, no clear conclusion can be drawn. The smaller blue and red ellipses, on the other hand, indicate the discrimination power of the future LHC and ILC/GigaZ measurements. With the improved precision a small part of the MSSM parameter space could be singled out.

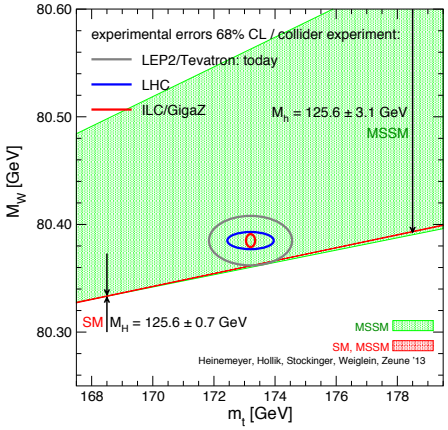

Figure 1-3. *Predictions for M_W as a function of m_t in the SM and MSSM (see text). The gray, blue and red ellipses denote the current, LHC and ILC/GigaZ precision, respectively.*

In a second step we apply the precise ILC measurement of M_W to investigate its potential to determine unknown model parameters. Within the MSSM we assume the hypothetical future situation that a light scalar top has been discovered with $m_{\tilde{t}_1} = 400 \pm 40$GeV at the LHC, but that no other new particle has been observed. We set lower limits of 300GeV on sleptons, charginos and neutralinos, 500GeV on other scalar quarks of the third generation and of 1500GeV on the remaining colored particles. We have selected the points from our scan accordingly. Any additional particle observation would lead to an even more restricted set of points and thus strengthen the parameter determination. In Fig. 1-4, we show the "surviving" points from our scan. All points fulfil $M_h = 125.8 \pm 3.1$GeV and $m_{\tilde{t}_1} = 400 \pm 40$GeV. Orange, red and blue points have in addition a W boson mass of $M_W = 80.375, 80.385, 80.395 \pm 0.005$GeV, respectively. In the figure we show the results for the heavy scalar top and the light scalar bottom. It can be seen that these unknown mass scales are restricted to small intervals if 80.385GeV or 80.395GeV are assumed as central experimental values (i.e. sufficiently different from the SM prediction). In this situation the precise M_W measurement could give clear indications where to search for these new particles (or how to rule out the simple MSSM picture).

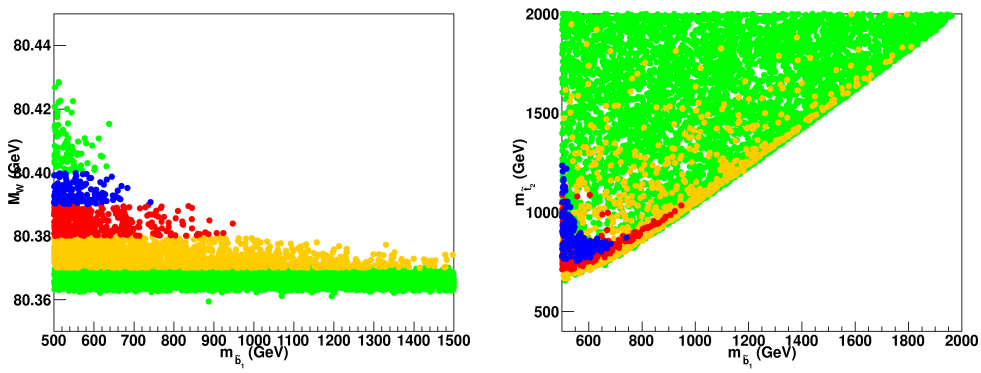

Figure 1-4. *Results of a MSSM parameter scan to illustrate what can be learned from an improved M_W measurement under the assumption a light stop is found with $m_{\tilde{t}_1} = 400 \pm 40$ GeV: green points: all points in the scan with $M_h = 125.64 \pm 3.08$ GeV and $m_{\tilde{t}_1} = 400 \pm 40$ GeV, yellow,red,blue points: $M_W = 80.385 \pm 0.005$ GeV (red), $M_W = 80.375 \pm 0.005$ GeV (yellow), and $M_W = 80.395 \pm 0.005$ GeV (blue).*

As for M_W the MSSM parameter space could also be constrained by a precise measurement of $\sin^2\theta^\ell_{\rm eff}$. The evaluation of the latter is performed at the same level of accuracy as for M_W [152].

In the first example it is investigated whether the high accuracy achievable at the GigaZ option of the ILC would provide sensitivity to indirect effects of SUSY particles even in a scenario where the superpartners are so heavy that they escape detection at the LHC [152]. We consider in this context a scenario with very heavy squarks and a very heavy gluino. It is based on the values of the SPS 1a′ benchmark scenario [36], but the squark and gluino mass parameters are fixed to 6 times their SPS 1a′ values. The other masses are scaled with a common scale factor given by the light chargino mass, except M_A which we keep fixed at its SPS 1a′ value. In this scenario the strongly interacting particles are too heavy to be detected at the LHC, while, depending on the scale-factor, some colour-neutral particles may be in the ILC reach. In Fig. 1-5 we show the prediction for $\sin^2\theta^\ell_{\rm eff}$ in this scenario as a function of the lighter chargino mass, $m_{\tilde{\chi}_1^\pm}$. The prediction includes the parametric uncertainty, $\sigma^{\rm para-LC}$, induced by the ILC measurement of m_t, $\Delta m_t = 100$MeV, and the numerically more relevant prospective future uncertainty on $\Delta\alpha^{(5)}_{\rm had}$, $\delta(\Delta\alpha^{(5)}_{\rm had}) = 5 \times 10^{-5}$. The MSSM prediction for $\sin^2\theta^\ell_{\rm eff}$ is compared with the experimental resolution with GigaZ precision, $\sigma^{\rm LC} = 0.000013$, using for simplicity the current experimental central value. The SM prediction (with $M_H^{\rm SM} = M_h^{\rm MSSM}$) is also shown, applying again the parametric uncertainty $\sigma^{\rm para-LC}$. Despite the fact that no coloured SUSY particles would be observed at the LHC in this scenario, the ILC with its high-precision measurement of $\sin^2\theta^\ell_{\rm eff}$ in the GigaZ mode could resolve indirect effects of SUSY up to $m_{\tilde{\chi}_1^\pm} \lesssim 500$GeV. This means that the high-precision measurements at the LC with GigaZ option could be sensitive to indirect effects of SUSY even in a scenario where SUSY particles have *neither* been directly detected at the LHC nor the first phase of the ILC with a centre of mass energy of up to 500GeV.

We now analyse the sensitivity of $\sin^2\theta^\ell_{\rm eff}$ together with M_W to higher-order effects in the MSSM by investigating a broad parameter scan range similar as in Tab. 1-13. Only the constraints on the MSSM parameter space from the LEP Higgs searches [154, 155] and the lower bounds on the SUSY particle masses previous to the LHC SUSY searches were taken into account. However, the SUSY particles strongly affected by the LHC searches are the squarks of the first and second generation and the gluino. Exactly these particles, however, have a very small effect on the prediction of M_W and $\sin^2\theta^\ell_{\rm eff}$ and thus a negligible effect on this analysis.

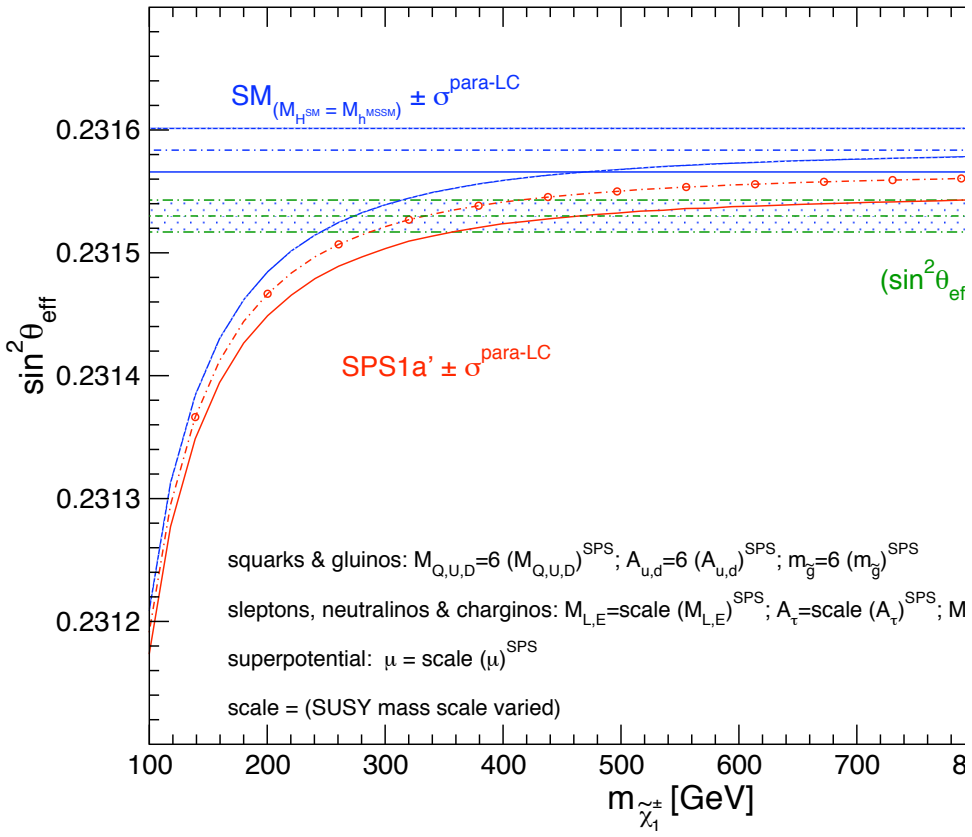

Figure 1-5. *Theoretical prediction for* $\sin^2\theta^\ell_{\rm eff}$ *in the SM and the MSSM (including prospective parametric theoretical uncertainties) compared to the experimental precision at the ILC with GigaZ option. An SPS 1a′ inspired scenario is used, where the squark and gluino mass parameters are fixed to 6 times their SPS 1a′ values. The other mass parameters are varied with a common scalefactor (see text).*

In Fig. 1-6 we compare the SM and the MSSM predictions for M_W and $\sin^2\theta^\ell_{\rm eff}$ as obtained from the scatter data. The predictions within the two models give rise to two regions in the M_W–$\sin^2\theta^\ell_{\rm eff}$ plane, red for the SM and green for the MSSM, where in fact the SM region also forms part of the MSSM allowed intervals in

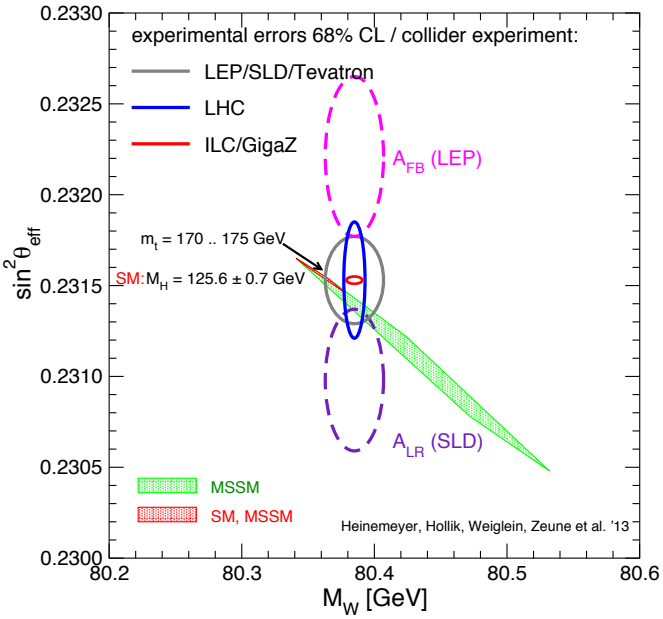

Figure 1-6. *MSSM parameter scan for M_W and $\sin^2\theta^\ell_{\rm eff}$ (see text). Todays 68% C.L. ellipses (from $A^b_{\rm FB}$(LEP), $A^e_{\rm LR}$(SLD) and the world average) are shown as well as the anticipated LHC and ILC/GigaZ precisions, drawn around todays central value.*

the decoupling regime. For the SM $M_H^{\rm SM} = 125.8 \pm 0.7$GeV has been required, whereas for the MSSM the Higgs mass measurement is met with a larger uncertainty due to the still large theory uncertainties in the M_h calculation [145]. The variation with m_t from 170...175GeV is indicated. The 68% C.L. experimental results for M_W and $\sin^2\theta^\ell_{\rm eff}$ are indicated in the plot, given for the current precision and for the anticpated LHC and ILC/GigaZ accuracies, see Tab. 1-12. The center ellipse corresponds to the current world average. Also shown are the error ellipses corresponding to the two individual most precise measurements of $\sin^2\theta^\ell_{\rm eff}$, based on $A^e_{\rm LR}$ by SLD and $A^b_{\rm FB}$ by LEP, corresponding to

$$A^b_{\rm FB}({\rm LEP}) \;:\; \sin^2\theta^{\ell\,{\rm exp,LEP}}_{\rm eff} = 0.23221 \pm 0.00029\ , \tag{1.14}$$

$$A^e_{\rm LR}({\rm SLD}) \;:\; \sin^2\theta^{\ell\,{\rm exp,SLD}}_{\rm eff} = 0.23098 \pm 0.00026\ , \tag{1.15}$$

$$\sin^2\theta^{\ell\,{\rm exp,aver.}}_{\rm eff} = 0.23153 \pm 0.00016\ , \tag{1.16}$$

where the latter one represents the average [**?**]. The first (second) value prefers a value of $M_H^{\rm SM} \sim 32(437)$GeV. The two measurements differ by more than $3\,\sigma$. The averaged value of $\sin^2\theta^\ell_{\rm eff}$, as given in Eq. 1.16, prefers $M_H^{\rm SM} \sim 110$GeV. One can see that the current averaged value is compatible with the SM with $M_H^{\rm SM} \sim 125.8$GeV and with the MSSM. The value of $\sin^2\theta^\ell_{\rm eff}$ obtained from $A^e_{\rm LR}$(SLD) clearly favors the MSSM over the SM. On the other hand, the value of $\sin^2\theta^\ell_{\rm eff}$ obtained from $A^b_{\rm FB}$(LEP) together with the M_W data from LEP and the Tevatron would correspond to an experimentally preferred region that deviates from the predictions of both models. This unsatisfactory solution can only be resolved by new measurements. The anticipated LHC accuracy for $\sin^2\theta^\ell_{\rm eff}$ would have only a limited potential to resolve this discrepancy, as it is larger than the current uncertainty obtained from the LEP/SLD average. On the other hand, a Z factory, i.e. the GigaZ option would be an ideal solution, as is indicated by the

red ellipse. The anticipated ILC/GigaZ precision of the combined M_W–$\sin^2\theta^\ell_{\rm eff}$ measurement could put severe constraints on each of the models and resolve the discrepancy between the $A^b_{\rm FB}$(LEP) and $A^e_{\rm LR}$(SLD) measurements. If the central value of an improved measurement with higher precision should turn out to be close to the central value favored by the current measurement of $A^b_{\rm FB}$(LEP), this would mean that the electroweak precision observables M_W and $\sin^2\theta^\ell_{\rm eff}$ could rule out both the SM and the most general version of the MSSM.

1.2.5 EWPO and Z'

Author: Jens Erler

EWPOs also constrain possible new physics scenarios such as $U(1)'$ gauge extensions of the SM. Current constraints [**?**] on the associated Z' boson masses, $M_{Z'}$, are generally comparable and in some cases stronger than the direct lower search limits from LEP and the Tevatron. The 8 TeV LHC data have extended the lower limits to roughly 2.5 TeV (depending on the model). However, the LHC dilepton and dijet resonance searches are insensitive to the Z-Z' mass mixing angle, $\theta_{ZZ'}$. Current EWPOs constrain $\theta_{ZZ'}$ to the 10^{-2} level and very often well below this. The EWPOs projected for the ILC with the GigaZ option as discussed above (most importantly the measurements of M_W to 2 MeV, the effective weak mixing angle to 1.3×10^{-5}, and m_t to 0.1 GeV) would improve the $\theta_{ZZ'}$ limits by almost another order of magnitude. This is important, since in specific models, $M_{Z'}$ and $\theta_{ZZ'}$ are not independent. As an example, consider the popular benchmark case of the Z_χ boson (appearing in $SO(10)$ GUT models) with a $U(1)'$ breaking Higgs sector compatible with supersymmetry. In this case, the projected EWPOs would experience noticeable shifts for $M_{Z'}$ values of up to 6 TeV, without assuming any improvement in $\Delta\alpha_{\rm had}$. The EWPOs are also important for leptophobic Z' bosons where the LHC sets weaker mass limits.

In the case of a Z' discovery at the LHC, it becomes mandatory to achieve the highest possible accuracy in the EWPOs. As an illustration, suppose a future LHC run discovers a dilepton resonance with an invariant mass of 3 TeV. Even if one would succeed to determine the spin of the resonance, it would not be possible to simultaneously obtain meaningful information on the coupling strength and on $\theta_{ZZ'}$, by using LHC data alone. But the EWPOs would determine the size and the sign of $\theta_{ZZ'}$ which would give valuable information on the $U(1)'$ breaking sector and *simultaneously* constraining the T parameter to the level of ±0.01, thereby constraining possible additional non-degenerate fermion (or scalar) multiplets that may be necessary to cancel gauge anomalies related to the $U(1)'$.

1.2.6 S,T, and U and BSM physics

Authors: GFITTER (Max Baak)

Goal: Update of previous studies to take into account Higgs mass constraint. Constraints on a number of BSM models from S,T,U in view of future improvements in the measurement of S,T,U. Illustration of scenarios where there is sensitivity even when no new physics is found at the LHC.

Examples: 2HDM, ED, Little Higgs, Technicolor

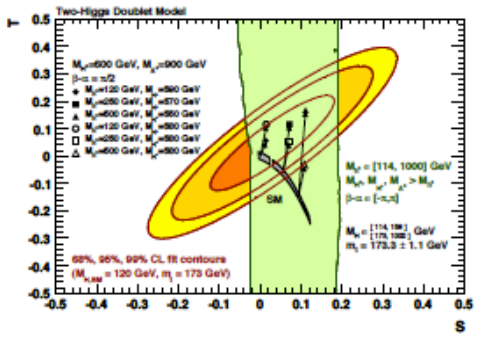

Figure 1-7. *Oblique paramters in the 2HDM. These studies are being updated by the GFITTER collaboration for Snowmass.*

1.3 Non-standard EW interactions in VBS and tri-boson processes and scales of new physics

Multi-boson production in various topologies provides a unique way to probe new physics. Assuming that the 125 GeV boson discovered at the LHC is the SM Higgs boson, it is natural to assume that electroweak symmetry breaking occurs according to the SM Higgs mechanism. Therefore, deviations from the SM in multi-boson production can be parameterized by SU(2)×U(1) operators which do not introduce any new sources of EWSB. If the new physics associated with these operators occurs at a high mass scale, one is motivated to use the formulation of Effective Field Theory (EFT) to organize the operators in order of increasing dimensionality.

As an example of new physics in the Higgs sector, let us consider the interaction of the Higgs field ϕ with a new scalar field S of the form $\phi^\dagger\phi S$. This operator can mediate $\phi\phi \to \phi\phi$ scattering via s and t channel exchange of the S boson. In the limit of the mass of S being much larger than the energy of this scattering process, the lowest dimension effective operator induced is the dimension-4 operator $(\phi^\dagger\phi)^2$, which mimics the quartic Higgs potential in the SM. At the next order in the momentum flowing along the S propagator, the effective operator induced is

$$O_{\phi d} = \frac{c_{\phi d}}{M_S^2}\partial_\mu(\phi^\dagger\phi)\partial^\mu(\phi^\dagger\phi)$$

where the coefficient is enhanced by the coupling of the ϕ to the S field and is suppressed by the squared mass of the S boson. This example illustrates a tree-level contribution to a higher-dimension operator due to a new interaction with a massive scalar field. After the Higgs field ϕ acquires a vev, the operator $O_{\phi d}$ changes the normalization of the Higgs field and therefore changes its coupling to the electroweak gauge bosons. As a result, the unitarization of the vector boson scattering amplitudes is altered and we would expect anomalous VBS.

An example of a dimension-8 operator is provided by the analogue of the QED light-by-light scattering mediated by the electron box loop. In the limit that the electromagnetic field is weak and slowly varying, this process is described by the Euler-Heisenberg Lagrangian

$$\mathcal{L}_{EH} = \frac{1}{2}(E^2 - B^2) + 2\frac{\alpha^2}{45m^4}((E^2 - B^2)^2 + 7(E.B)^2)$$

where E and B are the electric and magnetic field strengths, α is the electromagnetic coupling and m is the electron mass. The second term represents the $\gamma\gamma \to \gamma\gamma$ scattering EFT operator induced by the electron

box diagram when the photon energies are much smaller than the electron mass. This term can be re-written as a linear combination of $(F_{\mu\nu}F^{\mu\nu})^2$ and $(F_{\mu\rho}F^{\mu\sigma})(F^{\nu\rho}F_{\nu\sigma})$, where F is the electromagnetic field strength tensor.

Similarly, one may imagine a new heavy fermion coupling to the electroweak gauge bosons and inducing a four-boson contact interaction via a box loop. Such an interaction can mediate anomalous triple gauge boson production and anomalous vector boson scattering. The operator would be suppressed by four powers of the heavy fermion mass and enhanced by potentially strong coupling between the new fermion and the longitudinal vector bosons. These dimension-8 operators are described by the operators $\mathcal{O}_{T,i}, i = 0, 1, 2$ of Eqs. 1.39, 1.40 and 1.41.

1.3.1 Theory of non-standard gauge boson interactions

Authors: Oscar, Bastian, Juergen, Celine, Michael R., Olivier (white paper)

Electroweak vector boson pair and triple production and scattering are sensitive probes of the electroweak sector of the SM. They are sensitive to higher dimensional operators that affect electroweak gauge and Higgs boson couplings. In the following we will describe the EFT of new physics entering at energy scale Λ including dimension six and dimension eight operators,

$$\mathcal{L}_{\mathcal{EFT}} = \mathcal{L}_{SM} + \sum_i \frac{c_i}{\Lambda^2}\mathcal{O}_i + \sum_j \frac{f_j}{\Lambda^4}\mathcal{O}_j \tag{1.17}$$

and will discuss the potential of multi-boson processes for constraining some of these possible higher dimensional operators.

1.3.1.1 Dimension-six operators for electroweak vector boson pair and triple production and scattering

If baryon and lepton numbers are conserved, only operators with even dimension can be constructed. Consequently, the largest new physics contribution is expected from dimension-six operators. Three CP conserving dimension-six operators,

$$\begin{aligned} \mathcal{O}_{WWW} &= \mathrm{Tr}[W_{\mu\nu}W^{\nu\rho}W^{\mu}_{\rho}] \\ \mathcal{O}_{W} &= (D_\mu\Phi)^\dagger W^{\mu\nu}(D_\nu\Phi) \\ \mathcal{O}_{B} &= (D_\mu\Phi)^\dagger B^{\mu\nu}(D_\nu\Phi), \end{aligned} \tag{1.18}$$

and two CP violating dimension-six operators,

$$\begin{aligned} \mathcal{O}_{\tilde{W}WW} &= \mathrm{Tr}[\tilde{W}_{\mu\nu}W^{\nu\rho}W^{\mu}_{\rho}] \\ \mathcal{O}_{\tilde{W}} &= (D_\mu\Phi)^\dagger \tilde{W}^{\mu\nu}(D_\nu\Phi), \end{aligned} \tag{1.19}$$

affect the triple and quartic gauge couplings. Like in the SM, TGC and QGC from dimension-six operators are completely related to guarantee gauge invariance. In addition, three CP-conserving dimension-six operators

$$\mathcal{O}_{\phi d} = \partial_\mu \left(\phi^\dagger\phi\right) \partial^\mu \left(\phi^\dagger\phi\right) \tag{1.20}$$

$$\mathcal{O}_{\phi W} = \left(\phi^\dagger\phi\right) \mathrm{Tr}[W^{\mu\nu}W_{\mu\nu}] \tag{1.21}$$

$$\mathcal{O}_{\phi B} = \left(\phi^\dagger\phi\right) B^{\mu\nu}B_{\mu\nu} \tag{1.22}$$

modify the coupling of the Higgs to the weak gauge bosons and therefore the four-boson amplitudes [4]. The list of vertices relevant for three and four-boson amplitudes of each operator is displayed in Tab. 1-14.

	ZWW	AWW	HWW	HZZ	HZA	HAA	WWWW	ZZWW	ZAWW	AAWW
$\mathcal{O}_{WWW}$	x	x					x	x	x	x
$\mathcal{O}_{W}$	x	x	x	x	x		x	x	x	
$\mathcal{O}_{B}$	x	x		x	x					
$\mathcal{O}_{\phi d}$			x	x						
$\mathcal{O}_{\phi W}$			x	x	x	x				
$\mathcal{O}_{\phi B}$				x	x	x				
$\mathcal{O}_{\tilde{W}WW}$	x	x					x	x	x	x
$\mathcal{O}_{\tilde{W}}$	x	x	x	x	x					

Table 1-14. *The vertices induced by each operator are marked with an x in the corresponding column. The vertices that are not relevant for three and four gauge boson amplitudes have been omitted.*

In the definitions of the operators we have used

$$D_\mu \equiv \partial_\mu - i\frac{g'}{2}B_\mu Y - ig_w W_\mu^i \frac{\tau^i}{2} - ig_s G_\mu^a T^a \tag{1.23}$$

and

$$\begin{aligned} W_{\mu\nu} &= \frac{i}{2}g\tau^I(\partial_\mu W_\nu^I - \partial_\nu W_\mu^I + g\epsilon_{IJK}W_\mu^J W_\nu^K) \\ B_{\mu\nu} &= \frac{i}{2}g'(\partial_\mu B_\nu - \partial_\nu B_\mu) \end{aligned} \tag{1.24}$$

with $\mathrm{Tr}[\tau^i\tau^j] = 2\delta^{ij}$. We have neglected the operators affecting the couplings of the boson to fermions as they can be measured in other processes like the Z decay. This is a minimal set of independent dimension-six operators relevant for three and four electroweak weak gauge boson amplitudes. Additional dimension-six operators invariant under the SM symmetries can be constructed but they are equivalent to a linear combination of the previous operators due to the equations of motion. Consequently, other basis of operators can be chosen. For example, the operators $Q_{\phi D}$ and $Q_{\phi WB}$ in [103] have been replaced in this paper by $\mathcal{O}_{\mathcal{W}}$ and $\mathcal{O}_{\mathcal{B}}$. Our basis avoid the otherwise necessary redefinition the masses of the gauge bosons and the mixing of the neutral vector bosons. The operator $\mathcal{O}_{\phi d}$ does not contain any gauge boson since $\phi^\dagger\phi$ is a singlet under all the SM gauge groups. However, it contribute to the Higgs fields kinetic term after ϕ has been replaced by its value in the unitary gauge $\left(0, \frac{v+h}{\sqrt{2}}\right)^T$,

$$\mathcal{O}_{\phi d} \ni v^2 \partial_\mu h \partial^\mu h, \tag{1.25}$$

and requires a renormalization of the higgs field,

$$h \to h(1 - \frac{C_{\phi d}}{\Lambda^2}v^2), \tag{1.26}$$

in the full Lagrangian. The Higgs couplings to all the particles including the electroweak gauge bosons are consequently multiplied by the same factor. $\mathcal{O}_{\phi W}$ and $\mathcal{O}_{\phi B}$ modify the kinetic term of the gauge bosons after the Higgs doublet has been replaced by its vev. Those two operators require then a renormalization

[4] We have neglected the two CP violating operators with the dual strength tensors as measuring CP violation in four-boson amplitude would be very challenging

of the gauge fields and the gauge couplings. As a matter of fact, their part proportional to v^2 is entirely absorbed by those redefinitions and can therefore be removed directly in the definition of the operators, i.e.

$$\mathcal{O}_{\phi W} = \left(\phi^\dagger\phi - v^2\right) \mathrm{Tr}[W^{\mu\nu}W_{\mu\nu}] \tag{1.27}$$

$$\mathcal{O}_{\phi B} = \left(\phi^\dagger\phi - v^2\right) B^{\mu\nu}B_{\mu\nu} \tag{1.28}$$

It is now clear that those operators affect only the vertices with one or two Higgs boson and not the TCG or the QGC.

1.3.1.2 Anomalous quartic couplings: dimension-eight operators

As can be seen in Table 1-14, the dimension–six operators giving rise to QGCs also exhibit TGCs. In order to separate the effects of the QGCs we shall consider effective operators that lead to QGCs without a TGC associated to them. Moreover, not all possible QGCs are generated by dimension–six operators, for instance, these operators do not give rise to quartic couplings among the neutral gauge bosons [5]. The lowest dimension operator that leads to quartic interactions but does not exhibit two or three weak gauge boson vertices is dimension eight[6]. The counting is straightfoward: one can get a weak boson field either from the covariant derivative of Φ or from the field strength tensor. In either case the vector field is accompanied by a VEV or a derivative. Therefore, genuine quartic vertices are of dimension 8 or higher.

The idea behind using dimension–eight operators for QGCs is that the anomalous QGCs are to be considered as a straw man to evaluate the LHC potential to study these couplings, without having any theoretical prejudice about their size. There are three classes of genuine QGC operators [105] which will be discussed separately in the following,

1. Operators containing just $D_\mu\Phi$:
This class contains two independent operators, *i.e.*

$$\mathcal{O}_{S,0} = \left[(D_\mu\Phi)^\dagger D_\nu\Phi\right] \times \left[(D^\mu\Phi)^\dagger D^\nu\Phi\right] , \tag{1.29}$$

$$\mathcal{O}_{S,1} = \left[(D_\mu\Phi)^\dagger D^\mu\Phi\right] \times \left[(D_\nu\Phi)^\dagger D^\nu\Phi\right] , \tag{1.30}$$

where Λ is a typical energy scale of the new physics and the Higgs covariant derivative is given by the expression above in Eq. 1.23. The operators $\mathcal{O}_{S,0}$ and $\mathcal{O}_{S,1}$ contain quartic $W^+W^-W^+W^-$, W^+W^-ZZ and $ZZZZ$ interactions that do not depend on the gauge boson momenta; for a comparative table showing all QGCs induced by dimension–eight operators see table 1.3.1.2. In our framework, the QGCs are accompanied by vertices with more than 4 particles due to gauge invariance. In order to simply rescale the SM quartic couplings containing $W^\pm$ and Z it is enough to choose $f_{S0} = -f_{S1} = f$ that leads to SM quartic ouplings modified by a factor $(1 + fv^4/8)$, where v is the Higgs vaccum expectation value ($v \simeq 256$ GeV).

2. Operators containing $D_\mu\Phi$ and field strength:
QGCs are also generated by considering two electroweak field strength tensors and two covariant derivatives of the Higgs doublet [105]:

$$\mathcal{O}_{M,0} = \mathrm{Tr}\left[W_{\mu\nu}W^{\mu\nu}\right] \times \left[(D_\beta\Phi)^\dagger D^\beta\Phi\right] , \tag{1.31}$$

[5] Notice that the lowest order operators leading to neutral TGCs are also of dimension eight.

[6] Effective operators possessing QCGs but TGCs can be generated at tree level by new physics at a higher scale [106], in contrast with operators containing TGCs that are generated at loop level.

$$\mathcal{O}_{M,1} = \mathrm{Tr}\left[W_{\mu\nu}W^{\nu\beta}\right] \times \left[(D_\beta\Phi)^\dagger D^\mu\Phi\right] , \quad (1.32)$$

$$\mathcal{O}_{M,2} = \left[B_{\mu\nu}B^{\mu\nu}\right] \times \left[(D_\beta\Phi)^\dagger D^\beta\Phi\right] , \quad (1.33)$$

$$\mathcal{O}_{M,3} = \left[B_{\mu\nu}B^{\nu\beta}\right] \times \left[(D_\beta\Phi)^\dagger D^\mu\Phi\right] , \quad (1.34)$$

$$\mathcal{O}_{M,4} = \left[(D_\mu\Phi)^\dagger W_{\beta\nu}D^\mu\Phi\right] \times B^{\beta\nu} , \quad (1.35)$$

$$\mathcal{O}_{M,5} = \left[(D_\mu\Phi)^\dagger W_{\beta\nu}D^\nu\Phi\right] \times B^{\beta\mu} , \quad (1.36)$$

$$\mathcal{O}_{M,6} = \left[(D_\mu\Phi)^\dagger W_{\beta\nu}W^{\beta\nu}D^\mu\Phi\right] , \quad (1.37)$$

$$\mathcal{O}_{M,7} = \left[(D_\mu\Phi)^\dagger W_{\beta\nu}W^{\beta\mu}D^\nu\Phi\right] , \quad (1.38)$$

where the field strengths $W_{\mu\nu}$ and $B_{\mu\nu}$ have been defined above in Eq. 1.24. In this class of effective operators the quartic gauge-boson interactions depend upon the momenta of the vector bosons due to the presence of the field strength in their definitions. Therefore, the Lorentz structure of these operators can not be reduced to the SM one. The complete list of quartic vertices modified by these operators can be found in Table 1.3.1.2.

3. Operators containing four field strength tensors:
The following operators containing four field strength tensors also lead to quartic anomalous couplings:

$$\mathcal{O}_{T,0} = \mathrm{Tr}\left[W_{\mu\nu}W^{\mu\nu}\right] \times \mathrm{Tr}\left[W_{\alpha\beta}W^{\alpha\beta}\right] , \quad (1.39)$$

$$\mathcal{O}_{T,1} = \mathrm{Tr}\left[W_{\alpha\nu}W^{\mu\beta}\right] \times \mathrm{Tr}\left[W_{\mu\beta}W^{\alpha\nu}\right] , \quad (1.40)$$

$$\mathcal{O}_{T,2} = \mathrm{Tr}\left[W_{\alpha\mu}W^{\mu\beta}\right] \times \mathrm{Tr}\left[W_{\beta\nu}W^{\nu\alpha}\right] , \quad (1.41)$$

$$\mathcal{O}_{T,5} = \mathrm{Tr}\left[W_{\mu\nu}W^{\mu\nu}\right] \times B_{\alpha\beta}B^{\alpha\beta} , \quad (1.42)$$

$$\mathcal{O}_{T,6} = \mathrm{Tr}\left[W_{\alpha\nu}W^{\mu\beta}\right] \times B_{\mu\beta}B^{\alpha\nu} , \quad (1.43)$$

$$\mathcal{O}_{T,7} = \mathrm{Tr}\left[W_{\alpha\mu}W^{\mu\beta}\right] \times B_{\beta\nu}B^{\nu\alpha} , \quad (1.44)$$

$$\mathcal{O}_{T,8} = B_{\mu\nu}B^{\mu\nu}B_{\alpha\beta}B^{\alpha\beta} \quad (1.45)$$

$$\mathcal{O}_{T,9} = B_{\alpha\mu}B^{\mu\beta}B_{\beta\nu}B^{\nu\alpha} . \quad (1.46)$$

It is interesting to notice that the two last operators $\mathcal{L}_{T,8}$ and $\mathcal{O}_{T,9}$ give rise to QGCs containing only the neutral electroweak gauge bosons.

	WWWW	WWZZ	ZZZZ	WWAZ	WWAA	ZZZA	ZZAA	ZAAA	AAAA
$\mathcal{O}_{S,0}$, $\mathcal{O}_{S,1}$	X	X	X						
$\mathcal{O}_{M,0}$, $\mathcal{O}_{M,1}$,$\mathcal{O}_{M,6}$,$\mathcal{O}_{M,7}$	X	X	X	X	X	X	X		
$\mathcal{O}_{M,2}$,$\mathcal{O}_{M,3}$, $\mathcal{O}_{M,4}$,$\mathcal{O}_{M,5}$		X	X	X	X	X	X		
$\mathcal{O}_{T,0}$,$\mathcal{O}_{T,1}$,$\mathcal{O}_{T,2}$	X	X	X	X	X	X	X	X	X
$\mathcal{O}_{T,5}$,$\mathcal{O}_{T,6}$,$\mathcal{O}_{T,7}$		X	X	X	X	X	X	X	X
$\mathcal{O}_{T,8}$,$\mathcal{O}_{T,9}$			X			X	X	X	X

Table 1-15. *Quartic vertices modified by each dimension-8 operator are marked with X.*

1.3.1.3 Conventions for non-standard electroweak gauge boson interactions in different programs

Dimension-8 operators: VBFNLO and MadGraph5

The convention for the dimension-8-operators in VBFNLO is just the same as described in Section 1.3.1.2, and the coefficients f_i/Λ^4 set in the input file are just the ones of Equations A, B and C. However, the MadGraph5 implementation by means of a UFO file [138] uses expressions for the field strengths which are slightly different than the ones from Eq. 1.24:

$$\begin{aligned} W_{\mu\nu} &= \frac{1}{2}\tau^I(\partial_\mu W^I_\nu - \partial_\nu W^I_\mu + g\epsilon_{IJK}W^J_\mu W^K_\nu) \\ B_{\mu\nu} &= (\partial_\mu B_\nu - \partial_\nu B_\mu) \end{aligned} \tag{1.47}$$

The resulting changes can be absorbed in a redefinition of the operator coefficients:

$$\begin{aligned} f_{S,0,1} = f^{\mathrm{VBFNLO}}_{S,0,1} &= f^{\mathrm{MG5}}_{S,0,1} \\ f_{M,0,1} = f^{\mathrm{VBFNLO}}_{M,0,1} &= -\frac{1}{g^2}\cdot f^{\mathrm{MG5}}_{M,0,1} \\ f_{M,2,3} = f^{\mathrm{VBFNLO}}_{M,2,3} &= -\frac{4}{g'^2}\cdot f^{\mathrm{MG5}}_{M,2,3} \\ f_{M,4,5} = f^{\mathrm{VBFNLO}}_{M,4,5} &= -\frac{2}{gg'}\cdot f^{\mathrm{MG5}}_{M,4,5} \\ f_{M,6,7} = f^{\mathrm{VBFNLO}}_{M,6,7} &= -\frac{1}{g^2}\cdot f^{\mathrm{MG5}}_{M,6,7} \\ f_{T,0,1,2} = f^{\mathrm{VBFNLO}}_{T,0,1,2} &= \frac{1}{g^4}\cdot f^{\mathrm{MG5}}_{T,0,1,2} \\ f_{T,5,6,7} = f^{\mathrm{VBFNLO}}_{T,5,6,7} &= \frac{4}{g^2g'^2}\cdot f^{\mathrm{MG5}}_{T,5,6,7} \\ f_{T,8,9} = f^{\mathrm{VBFNLO}}_{T,8,9} &= \frac{16}{g'^4}\cdot f^{\mathrm{MG5}}_{T,8,9} \end{aligned} \tag{1.48}$$

Dimension-8 operators: WHIZARD

As WHIZARD uses different anomalous couplings operators than the ones described in Section 1.3.1.2, assuming a different symmetry group [**?**], a conversion is in general not possible. However, a vertex-specific conversion exists for the operators $\mathcal{L}_{S,0}$ and $\mathcal{L}_{S,1}$ to their corresponding operators

$$\mathcal{L}^{(4)}_4 = \alpha_4 \left[\mathrm{Tr}\left(\mathrm{V}_\mu \mathrm{V}_\nu\right)\right]^2 \tag{1.49}$$

$$\mathcal{L}^{(4)}_5 = \alpha_5 \left[\mathrm{Tr}\left(\mathrm{V}_\mu \mathrm{V}^\mu\right)\right]^2, \quad \text{with } \mathrm{V}_\mu = \left(\mathrm{D}_\mu \Sigma\right)\Sigma^\dagger\ . \tag{1.50}$$

The conversion reads:

- for the WWWW-Vertex:

$$\alpha_4 = \frac{f_{S0}}{\Lambda^4}\frac{v^4}{8} \tag{1.51}$$

$$\alpha_4 + 2\cdot\alpha_5 = \frac{f_{S1}}{\Lambda^4}\frac{v^4}{8} \tag{1.52}$$

- for the WWZZ-Vertex:

$$\alpha_4 = \frac{f_{S0}}{\Lambda^4}\frac{v^4}{16} \tag{1.53}$$

$$\alpha_5 = \frac{f_{S1}}{\Lambda^4}\frac{v^4}{16} \tag{1.54}$$

- for the ZZZZ-Vertex:

$$\alpha_4 + \alpha_5 = \left(\frac{f_{S0}}{\Lambda^4} + \frac{f_{S1}}{\Lambda^4}\right)\frac{v^4}{16} \tag{1.55}$$

Dimension-8 operators: Relations to LEP parametrization

The LEP constrains on the vertices $\gamma\gamma W^+W^-$ and $\gamma\gamma ZZ$ [107] described in terms of couplings a_0/Λ^2 and a_c/Λ^2 can be translated into bounds on $f_{M,0}$, $f_{M,1}$, $f_{M,2}$, and $f_{M,3}$ (in the conventions from Eq. 1.24) via the vertex-specific relations

- for the $WW\gamma\gamma$-Vertex:

$$\frac{f_{M,0}}{\Lambda^4} = \frac{a_0}{\Lambda^2}\frac{1}{g^2v^2} \quad \text{and} \quad \frac{f_{M,2}}{\Lambda^4} = \frac{a_0}{\Lambda^2}\frac{2}{g^2v^2} \tag{1.56}$$

$$\frac{f_{M,1}}{\Lambda^4} = -\frac{a_c}{\Lambda^2}\frac{1}{g^2v^2} \quad \text{and} \quad \frac{f_{M,3}}{\Lambda^4} = -\frac{a_c}{\Lambda^2}\frac{2}{g^2v^2} \tag{1.57}$$

- for the $ZZ\gamma\gamma$-Vertex:

$$\frac{f_{M,0}}{\Lambda^4} = \frac{a_0}{\Lambda^2}\frac{c_W^4}{g^2v^2} \quad \text{and} \quad \frac{f_{M,2}}{\Lambda^4} = \frac{a_0}{\Lambda^2}\frac{2c_W^4}{g^2v^2} \tag{1.58}$$

$$\frac{f_{M,1}}{\Lambda^4} = -\frac{a_c}{\Lambda^2}\frac{c_W^4}{g^2v^2} \quad \text{and} \quad \frac{f_{M,3}}{\Lambda^4} = -\frac{a_c}{\Lambda^2}\frac{2c_W^4}{g^2v^2} \tag{1.59}$$

where s_W (c_W) stands for the sine (cosine) of the weak mixing angle.

Dimension-6 operators: MadGraph5

The Madgraph model EWdim6 has been generated from FeynRules and contains the operators whose names and coefficients are displayed in Tab. 1-16. All the coefficients include the $1/\Lambda^2$ as reminded by the "L2" at the end of the names and are in TeV^{-2}. The model also has a new coupling order NP counting the power of $1/\Lambda$. Consequently, each vertex from the dimension-six operators has NP=2.

c_{WWW}/Λ^2	CWWWL2
c_W/Λ^2	CWL2
c_B/Λ^2	CBL2
$c_{\tilde{W}WW}/\Lambda^2$	CPWWWL2
$c_{\tilde{W}}/\Lambda^2$	CPWL2
$c_{\phi d}/\Lambda^2$	CphidL2
$c_{\phi W}/\Lambda^2$	CphiWL2
$c_{\phi B}/\Lambda^2$	CphiBL2

Table 1-16. *Names of the coupling of the dimension-six operators present in the EWdim6 model.*

Dimension-6 operators: VBFNLO

The operators $\mathcal{O}_{WWW}$, $\mathcal{O}_W$, $\mathcal{O}_B$, $\mathcal{O}_{\tilde{W}WW}$ and $\mathcal{O}_{\tilde{W}}$ from Equations 1.18, 1.19 and 1.22 from Section 1.3.1.1 are directly available in VBFNLO. The operator $\mathcal{O}_{\phi B}$ is called $\mathcal{O}_{BB}$ within VBFNLO. Additionally, the operator $\mathcal{O}_{WW}$ from VBFNLO can be related to the operator $\mathcal{O}_{\phi W}$ by choosing the coefficients as

$$f_{WW} = 2 \cdot c_{\phi W} \tag{1.60}$$

The $\mathcal{CP}$-conserving anomalous couplings implementation can also be used with the parameters Δg_1^Z, $\Delta\kappa_Z$, $\Delta\kappa_\gamma$ and , λ_γ, defined in Section 1.3.1.4.

1.3.1.4 Comparison with the anomalous coupling approach

The anomalous couplings approach for TGCs is based on the Lagrangian [102]

$$\begin{aligned}\mathcal{L} = ig_{WWV}\Big(&g_1^V(W^+_{\mu\nu}W^{-\mu} - W^{+\mu}W^-_{\mu\nu})V^\nu + \kappa_V W^+_\mu W^-_\nu V^{\mu\nu} + \frac{\lambda_V}{M_W^2}W^{\nu+}_\mu W^{-\rho}_\nu V^\mu_\rho \\ &+ig_4^V W^+_\mu W^-_\nu(\partial^\mu V^\nu + \partial^\nu V^\mu) - ig_5^V\epsilon^{\mu\nu\rho\sigma}(W^+_\mu\partial_\rho W^-_\nu - \partial_\rho W^+_\mu W^-_\nu)V_\sigma \\ &+\tilde{\kappa}_V W^+_\mu W^-_\nu \tilde{V}^{\mu\nu} + \frac{\tilde{\lambda}_V}{m_W^2}W^{\nu+}_\mu W^{-\rho}_\nu \tilde{V}^\mu_\rho\Big)\end{aligned} \tag{1.61}$$

where $V = \gamma, Z$; $W^\pm_{\mu\nu} = \partial_\mu W^\pm_\nu - \partial_\nu W^\pm_\mu$, $V_{\mu\nu} = \partial_\mu V_\nu - \partial_\nu V_\mu$, $g_{WW\gamma} = -e$ and $g_{WWZ} = -e\cot\theta_W$. The first three terms of Eq. (1.61) are C and P invariant while the remaining four terms violate C and/or P. Electromagnetic gauge invariance requires that $g_1^\gamma = 1$ and $g_4^\gamma = g_5^\gamma = 0$. Finally there are five independent C- and P-conserving parameters: $g_1^Z, \kappa_\gamma, \kappa_Z, \lambda_\gamma, \lambda_Z$; and six C and/or P violating parameters: $g_4^Z, g_5^Z, \tilde{\kappa}_\gamma, \tilde{\kappa_Z}, \tilde{\lambda}_\gamma, \tilde{\lambda_Z}$. This Lagrangian is not the most generic one as extra derivatives can be added in all the operators. Futhermore, there is no reason to remove those extra terms since they are not suppressed by Λ but by m_W.

The effective field theory approach described in the previous section allows one to calculate those parameters in terms of the coefficients of the five dimension-six operators relevant for TGC. Calling these coefficients $c_{WWW}, c_W, c_B, c_{\tilde{W}WW}, c_{\tilde{W}}$, one finds [101, 104]

$$g_1^Z = 1 + c_W\frac{m_Z^2}{2\Lambda^2} \tag{1.62}$$

$$\kappa_\gamma = 1 + (c_W + c_B)\frac{m_W^2}{2\Lambda^2} \tag{1.63}$$

$$\kappa_Z = 1 + (c_W - c_B\tan^2\theta_W)\frac{m_W^2}{2\Lambda^2} \tag{1.64}$$

$$\lambda_\gamma = \lambda_Z = c_{WWW}\frac{3g^2m_W^2}{2\Lambda^2} \tag{1.65}$$

$$g_4^V = g_5^V = 0 \tag{1.66}$$

$$\tilde{\kappa}_\gamma = c_{\tilde{W}}\frac{m_W^2}{2\Lambda^2} \tag{1.67}$$

$$\tilde{\kappa}_Z = -c_{\tilde{W}}\tan^2\theta_W\frac{m_W^2}{2\Lambda^2} \tag{1.68}$$

$$\tilde{\lambda}_\gamma = \tilde{\lambda}_Z = c_{\tilde{W}WW}\frac{3g^2m_W^2}{2\Lambda^2} \tag{1.69}$$

Defining $\Delta g_1^Z = g_1^Z - 1$, $\Delta\kappa_{\gamma,Z} = \kappa_{\gamma,Z} - 1$, the relation [101]

$$\Delta g_1^Z = \Delta\kappa_Z + \tan^2\theta_W\Delta\kappa_\gamma \tag{1.70}$$

and the relation $\lambda_\gamma = \lambda_Z$ reduce the five C and P violating parameters down to three. For the C and/or P violating parameters, the relation

$$0 = \tilde{\kappa}_Z + \tan^2\theta_W \tilde{\kappa}_\gamma \tag{1.71}$$

and the relations $\tilde{\lambda}_\gamma = \tilde{\lambda}_Z$ and $g_4^Z = g_5^Z = 0$ reduce the six C and/or P violating parameters down to just two.

The Lagrangian 1.61 is not $SU(2)_L$ gauge invariant even after imposing those relation because the quartic and higher multiplicity couplings are not included. Furthermore, gauge invariance requires also several relations between vertices with different number of particles. Therefore, the anomalous coupling Lagrangian cannot be used for four gauge bosons amplitudes.

The quartic couplings involving two photons have been parametrized in a similar way. However, the parametrization is not generic enough and does not include the contributions from the dimension-six operators.

1.3.1.5 Discussion of unitarity bounds and usage of form factors

The effective theory is valid only below the new physics scale and no violation of unitarity occurs in this area as illustrated by Fig. 1-8. As a matter of fact, the pure SM contribution, the interference with the dimension-six operators and the the square of the new physics amplitude are suppressed by increasing power of $1/\Lambda$,

$$|M_{SM} + M_{dim6} + \ldots|^2 = \underbrace{|M_{SM}|^2}_{\Lambda^0} + \underbrace{2\mathcal{R}e\,(M_{SM} M_{dim6})}_{\Lambda^{-2}} + \underbrace{|M_{dim6}|^2 + \ldots}_{\Lambda^{-4}}. \tag{1.72}$$

All those contributions have a similar magnitude for $m_{WW} \approx 1.3$ TeV on the right figure. Clearly, the $1/\Lambda$ expansion is only valid below this energy where unitarity is preserved as shown by the left figure.

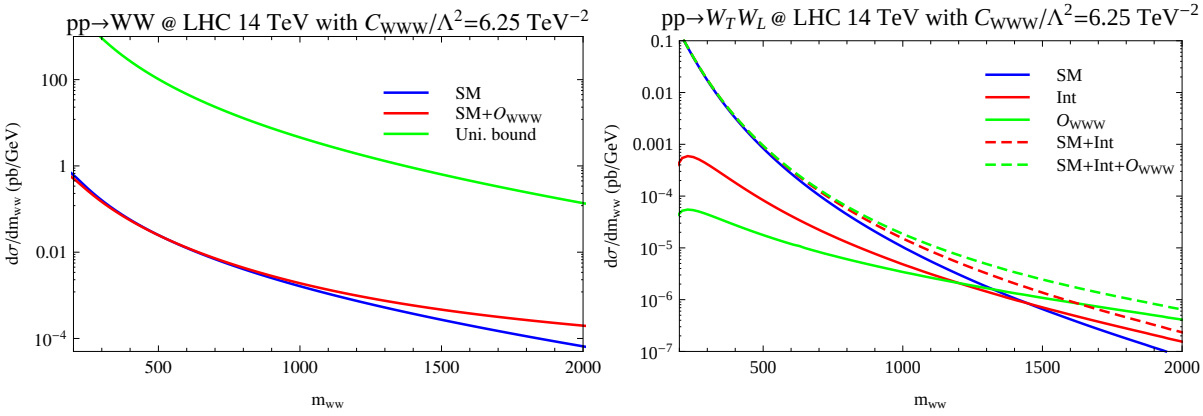

Figure 1-8. *The contribution of the SM (in blue) and of the SM and $\mathcal{O}_{WWW}$ for $c_{WWW}/\Lambda^2 = 6.25$ TeV (in red) to W pair production and the unitarity bound [99] (in green) are displayed on the left figure. The right figure shows the production of one longitudinally and one tranversally polarized W boson from the SM (solid blue line), from the interference between the SM and the dimension-six operator (solid red line), from the sum of the two (dashed red line), from the square of the new physics amplitude (solid green line) and finally the total contribution from the SM and the dimension-six operator.*

	σ_{LO}	σ_{NLO}
SM	1.169 fb	1.176 fb
anom.coupl.	1.399 fb	1.388 fb

Table 1-17. *Total cross sections at LO and NLO for the process $pp \to e^+\nu_e\mu^+\nu_\mu jj$ in the SM and with anomalous coupling $\frac{f_{T,1}}{\Lambda^4} = 200\mathrm{TeV}^{-4}$. Statistical errors from Monte Carlo integration are below the per mille level.*

1.3.2 The role of higher order QCD corrections in multi-boson processes at the LHC

Higher-order corrections play an important role for accurate predictions at the LHC. In the following section we study the impact of NLO QCD corrections in vector-boson fusion and triboson processes and how they impact the extraction of anomalous quartic gauge couplings. As example of these two process classes we take the processes W^+W^+jj and $W^+\gamma\gamma$, respectively. All results have been obtained with VBFNLO.

1.3.2.1 Vector-boson-fusion process W^+W^+jj

The production of a vector-boson pair via vector-boson fusion [120, 121, 122, 123] has a characteristic signature of two high-energetic, so-called tagging jets in the forward region of the detector, which are defined as the two jets with the largest transverse momentum. This can be exploited experimentally by requiring that there is a large rapidity separation ($\Delta\eta_{jj} > 4$) between the tagging jets, they are in opposite detector hemispheres ($\eta_{j_1} \times \eta_{j_2} < 0$) and they possess a large invariant mass ($M_{jj} > 600$ GeV). Additional central jet radiation at higher orders is strongly suppressed due to the exchange of a color-singlet in the t-channel, in contrast to typical QCD-induced backgrounds. Higher-order corrections are typically small, below the 10% level, and reduce the residual scale uncertainty to about 2.5%. Choosing the momentum transfer between an incoming and an outgoing parton along a fermion line proves to be particularly advantageous, as then also corrections to important distributions are small and flat over the whole range.

As example we take the process $pp \to e^+\nu_e\mu^+\nu_\mu jj$ with anomalous coupling $\frac{f_{T,1}}{\Lambda^4} = 200\mathrm{TeV}^{-4}$ and formfactor scale $\Lambda = 1188$ GeV and exponent $p = 4$. The results for the total cross sections at LO and NLO are shown in Tab. 1-17. Switching on the anomalous couplings increases the cross section by just under 20%, and NLO QCD corrections hardly change this number. This can also be seen in Fig. 1-9 where we show the differential distribution with respect to the invariant mass of the two leptons and the two neutrinos. In the left-hand plot we present the differential cross section in the SM and with anomalous coupling switched on both at LO and NLO. Similar to the integrated cross section, the difference between LO and NLO is small in both cases. In contrast the anomalous couplings yield a positive contribution to the cross section over the SM, which starts at an invariant mass of about 500 GeV, before the formfactor, introduced to preserve unitarity, damps the contributions again at higher invariant masses. On the right-hand side we present two groups of ratios. The differential K factor is flat and close to one both for the SM and the anomalous coupling scenario. The second set shows the ratio of differential anomalous-coupling over SM cross section both at LO and NLO. The two curves agree well and show enhancements of the cross section up to a factor of three. Hence, in this process higher-order corrections do not influence the extraction of anomalous couplings.

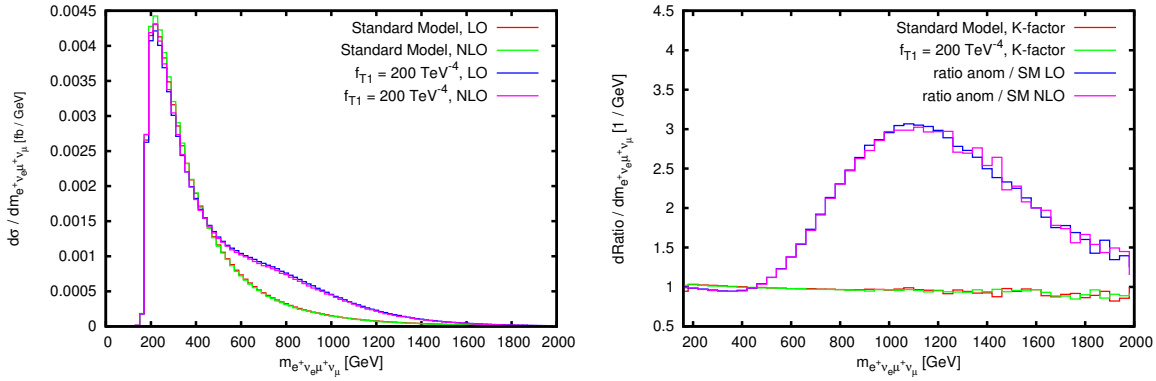

Figure 1-9. *Invariant-mass distribution of the two lepton, two neutrino system. Left: Differential cross section for the SM and with anomalous coupling T_1 at LO and NLO. Right: Differential K-factors for the SM and with anomalous coupling as well as the cross-section ratio between anomalous coupling and SM for LO and NLO.*

	σ_{LO}	σ_{NLO}
SM	1.124 fb	3.674 fb
anom.coupl.	1.216 fb	3.787 fb

Table 1-18. *Total cross sections at LO and NLO for the process $pp \to e^+\nu_e\gamma\gamma$ in the SM and with anomalous coupling $\frac{f_{T,6}}{\Lambda^4} = 2000\text{TeV}^{-4}$. Statistical errors from Monte Carlo integration are below the per mille level.*

1.3.2.2 Triboson process $W^+\gamma\gamma$

The second group of processes where anomalous quartic gauge couplings can be tested are the triboson processes [124, 125, 126, 127, 128, 129, 130, 131, 132, 133]. The quartic vertex enters via an s-channel vector boson, which decays into three vector bosons, while diagrams with two or three bosons attached to the quark line as well as non-resonant contributions form an irreducible background. These processes have been shown to possess quite large K factors, typically between 1.5 and 1.8, mostly due to the additional quark-gluon–induced production processes first entering in the real-emission process. They also have a considerable scale dependence. While the dependence on the factorization scale can be reduced by NLO QCD corrections, the strong coupling constant first enters in the real emission part and therefore shows a large variation with the scale.

The example process we are considering here is $pp \to e^+\nu_e\gamma\gamma$ [130, 131]. In this process the K factor with a numerical value of about 3 is particularly large. This is due to the fact that the SM amplitude vanishes when the two photons are collinear and $\cos\theta_W = \frac{1}{3}$, where θ_W is the angle between the W and the incoming quark in the partonic center-of-mass frame. This so-called radiation zero [134, 135, 136] is spoiled by the extra jet emission at NLO, therefore giving huge K factors in these phase-space regions. The numerical values for the integrated cross section are tabulated in Table 1-18. As anomalous coupling we choose the operator T_6 with $\frac{f_{T,6}}{\Lambda^4} = 2000\text{TeV}^{-4}$, formfactor scale $\Lambda = 1606$ GeV and exponent $p = 4$.

Turning to differential distributions, we show the transverse momentum distribution of the harder photon in Figure 1-10. The left-hand side shows again the differential integrated cross section. Both the SM and the anomalous-coupling scenario show differential NLO cross sections which are significantly larger than their

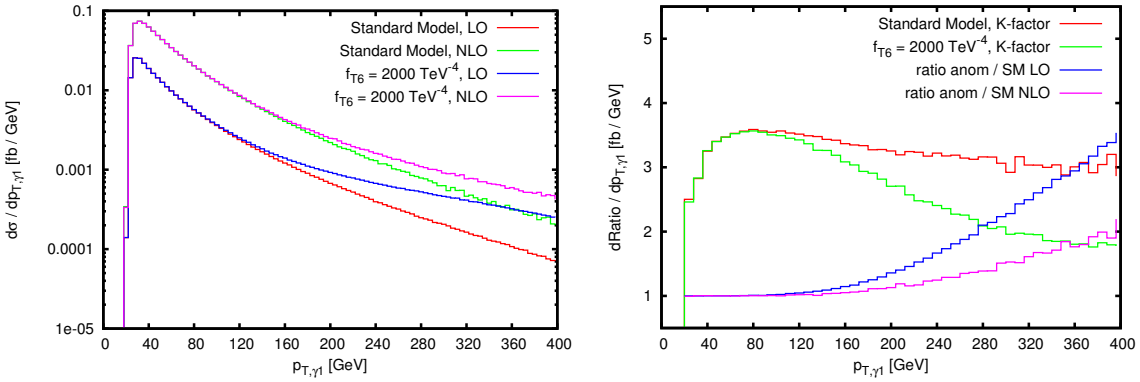

Figure 1-10. *Transverse-momentum distribution of the harder photon. Left: Differential cross section for the SM and with anomalous coupling T_6 at LO and NLO. Right: Differential K-factors for the SM and with anomalous coupling as well as the cross-section ratio between anomalous coupling and SM for LO and NLO.*

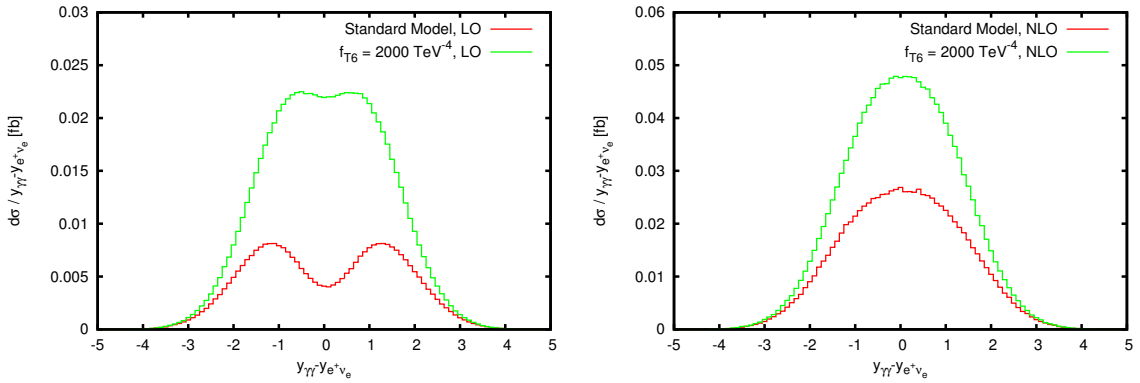

Figure 1-11. *Rapidity difference of the diphoton system and the lepton-neutrino system for the SM and the anomalous coupling scenario. Left: LO distributions Right: NLO distributions*

LO counterpart. Contributions from anomalous couplings start to contribute for transverse photon momenta above 100 GeV and their relative size becomes gradually larger when going to higher momenta as expected.

On the right-hand side one can see that the K-factor behavior differs for the SM and the anomalous coupling scenario. While, in the SM, the K factor is almost constant and only slightly decreases when going to larger transverse momenta, there is a much stronger decrease when anomalous couplings are switched on. At the high end of the shown range, the K factor has reached a value of around 1.8, which is the number typically observed in other triboson processes involving Ws. As the effect of the anomalous coupling increases, the cancellation between different amplitudes gets gradually destroyed and the radiation zero filled up. Only the effects from additional jet radiation remain, yielding the smaller K factor.

That this is indeed the case can be seen in Fig. 1-11. Here we require additionally that the transverse momentum of the harder photon exceeds 200 GeV and the invariant mass of the lepton-neutrino system exceeds 75 GeV to suppress radiation off the final-state lepton. The effect of the radiation zero should be visible as a dip at zero in the rapidity difference between the diphoton system and the lepton-neutrino system, which can be indeed observed for the LO SM curve. In contrast the anomalous-coupling curve shows no such behavior even at LO, and at NLO the dip is filled in both cases.

Turning back to the right-hand plot of Fig. 1-10, the ratio between anomalous-coupling and SM prediction decreases when going from LO to NLO. This is due to the same effect, as part of the additional contribution is caused by filling up the radiation zero, which is no longer present at NLO because there already QCD effects have caused this. Hence, for this process group, higher-order corrections play an important role and cannot be neglected when determining the size of or limits on anomalous quartic gauge couplings.

1.3.3 Current bounds on triple and quartic gauge boson couplings

Current bounds on aTGCs from LEP, Tevatron and LHC searches are presented in Figs. 1-12 and 1-13.

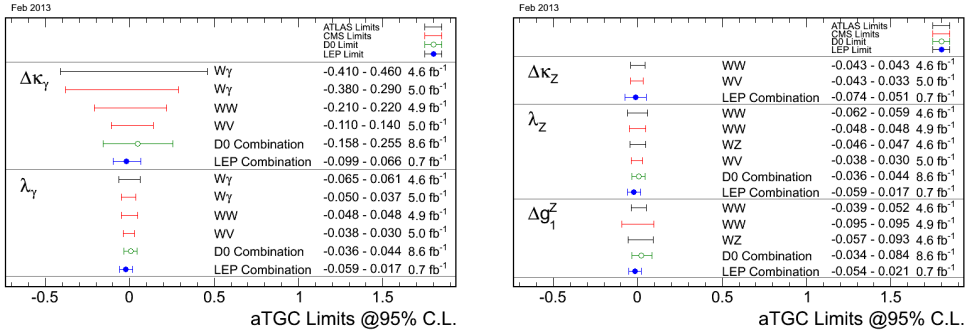

Figure 1-12. *Limits on anomalous $WW\gamma$ (l.h.s) and WWZ (r.h.s) couplings. Tevatron limits use a form factor with $\Lambda = 2$ TeV. Taken from Ref. [166].*

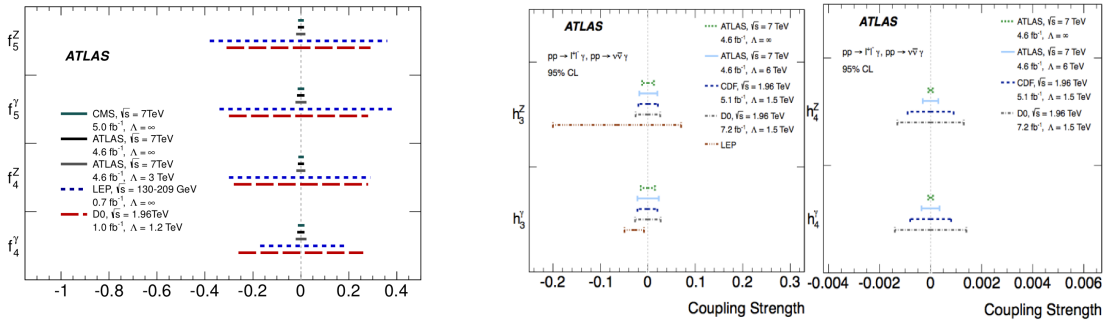

Figure 1-13. *Limits on $ZZ\gamma$ and ZZZ couplings from $Z\gamma$ (l.h.s) and ZZ (r.h.s) production processes. Tevatron limits use a form factor with $\Lambda = 1.5$ TeV. Taken from Ref. [166].*

1.3.4 Multi-boson processes at the 14 TeV LHC

Studies on vector boson scattering (VBS) and triboson production have been presented by ATLAS collaboration for $\sqrt{s} = 14$ TeV and integrated luminosities of 300 fb^{-1} and 3 ab^{-1} respectively. These studies showcase the greatly increased sensitivity for new physics in these channels.

Table 1-19. *Summary of expected upper limits for a_4 at the 95% confidence level using the $pp \to WW + 2j \to e\mu + 2j$ search at pp collision center-of-mass energy of 14 TeV.*

model	300 fb^{-1}	1 ab^{-1}	3 ab^{-1}
a_4	0.066	0.025	0.016

Studies of vector boson scattering in the $W^+W^-jj \to \ell\nu\ell\nu jj$ have been presented based on the comparison of the m_{lljj} distribution from backgrounds (including $t\bar{t}$ production, diboson production with ISR jets, and SM VBS) and anomalous VBS signal. The statistical sensitivity has been parameterized using the electroweak chiral lagrangian operator with coefficient α_4. In this formulation of new physics, this particular operator is one of the least constrained since it preserves the CP symmetry and the electoweak SU(2) custodial symmetry, does not induce oblique corrections in the gauge boson propagators, and only induces anomalous quartic couplings which have not been constrained by past studies on trilinear quage couplings. Unitarity is maintained by using the inverse amplitude method. Table 1-19 shows the results of this ATLAS study, as reproduced from their report. The sensitivity to the a_4 coefficient is increased by more than a factor of 4 in the high-luminosity upgrade of the LHC.

ATLAS has also presented a study of VBS in the $ZZ \to 4\ell$ channel which has a clean and fully reconstructible final state. In this study, the K-matrix unitarization approach is used to model anomalous quartic couplings and unitarization is achieved by including TeV-scale resonances. Such resonances would be clearly visible in the 4ℓ invariant mass distribution. Table 1-20, reproduced from the ATLAS report, shows the statistical significance of potential resonant signals given the background-only hypothesis, for a number of resonance masses and couplings. The comparison of the two scenarios with integrated luminosities of 300 fb^{-1} and 3000 fb^{-1} respectively showcases the discovery potential of the high-luminosity upgrade.

ATLAS has estimated the precision on the measurement of the integrated cross section for the purely-electroweak SM process $pp \to ZZ + 2j \to 4\ell + 2j$. In the kinematic region where the tagging forward jets have $m_{jj} > 1$ TeV and the 4-lepton invariant mass $m_{4\ell} > 200(500)$ GeV, a statistical precision of 10(15)% is achievable with 3000 fb^{-1}, compared to 30(45)% with 300 fb^{-1}. Since a key prediction of the SM is that the Higgs boson unitarizes longitudinal VBS, it is important to make the definitive measurements of this cross section, which is only possible with the high-luminosity upgrade in this clean and robust channel.

Table 1-20. *Summary of the expected sensitivity to anomalous VBS signal, quoted in terms of the background-only p_0-value expected for signal+background. The p_0-value has been converted to the corresponding number of Gaussian σ in significance. These results are given for the $pp \to ZZ+2j \to \ell\ell\ell\ell+2j$ channel at $\sqrt{s} = 14$ TeV. The increase in significance with integrated luminosity is shown for different resonance masses and couplings g.*

model	300 fb^{-1}	3000 fb^{-1}
$m_{\text{resonance}} = 500$ GeV, $g = 1.0$	2.4σ	7.5σ
$m_{\text{resonance}} = 1$ TeV, $g = 1.75$	1.7σ	5.5σ
$m_{\text{resonance}} = 1$ TeV, $g = 2.5$	3.0σ	9.4σ

ATLAS has also shown sensitivity studies using the fully-leptonic decay modes of $W^\pm W^\pm$, WZ and ZZ channels in the VBS mode as well as triboson results in the $Z\gamma\gamma$ channel. These results are quoted in the language of EFT higher-dimension operators. The studies are performed in the kinematic regions where unitarity is perserved. In this context, ATLAS has studied one dimension-6 operator, $\mathcal{O}_{\phi W}$ of Eq. 1.27 and four dimension-8 operators, $\mathcal{O}_{S,0}$ of Eqs. 1.29 and $\mathcal{O}_{T,i}, i = 1, 8, 9$ of Eqs. 1.40,1.45,1.46. Their values for 5σ-significance discovery are summarised in Table 1-21, reproduced from the ATLAS report. The high-

luminosity upgrade increases the discovery potential for the operator coefficients by factors of 2-3, with further increases possible using analysis optimizations. If an anomaly is discovered with 300 fb^{-1}, the corresponding operator coefficient can be measured with a precision of 5% or better with 3000 fb^{-1} of integrated luminosity, allowing detailed studies of the underlying physics in this arena.

Parameter	dimension	channel	Λ_{UV} [TeV]	300 fb^{-1}		3000 fb^{-1}	
				5σ	95% CL	5σ	95% CL
$c_{\phi W}/\Lambda^2$	6	ZZ	1.9	34 TeV^{-2}	20 TeV^{-2}	16 TeV^{-2}	9.3 TeV^{-2}
f_{S0}/Λ^4	8	$W^{\pm}W^{\pm}$	2.0	10 TeV^{-4}	6.8 TeV^{-4}	4.5 TeV^{-4}	0.8 TeV^{-4}
f_{T1}/Λ^4	8	WZ	3.7	1.3 TeV^{-4}	0.7 TeV^{-4}	0.6 TeV^{-4}	0.3 TeV^{-4}
f_{T8}/Λ^4	8	$Z\gamma\gamma$	12	0.9 TeV^{-4}	0.5 TeV^{-4}	0.4 TeV^{-4}	0.2 TeV^{-4}
f_{T9}/Λ^4	8	$Z\gamma\gamma$	13	2.0 TeV^{-4}	0.9 TeV^{-4}	0.7 TeV^{-4}	0.3 TeV^{-4}

Table 1-21. *5σ-significance discovery values and 95% CL limits for coefficients of higher-dimension operators. Λ_{UV} is the unitarity violation bound corresponding to the sensitivity with 3000 fb^{-1} of integrated luminosity.*

The substantially improved sensitivity to these higher dimensional operators highlights the potential of the LHC to probe one of the most important aspects of the electroweak sector of the SM, namely, the unitarization of the vector boson scattering amplitudes by the Higgs mechanism. Since the "mexican hat" Higgs potential is essentially just a parameterization, a more "dynamical" explanation of this potential in terms of the Higgs' interaction with new scalar, vector or fermion fields involving strong dynamics can easily induce higher-dimension operators as precursors to the more complete theory of the Higgs sector.

Another example of the impact of the HL-LHC in studying the unitarization mechanism is provided by the improved sensitivity to the $O_{\phi d}$ operator of Eq. 1.20 shown in Table 1-22. The threshold of interest in the magnitude of this operator is provided by v^{-2} where v is the Higgs field's vacuum expectation value, thus $v^{-2} = 16$ TeV^{-2}. As the sensitivity to the magnitude of this operator falls below 16 TeV^{-2}, we obtain a direct test of the SM unitarization mechanism. Table 1-22 shows that this threshold is crossed by increasing the LHC integrated luminosity from 300 fb^{-1} to 3000 fb^{-1}.

Vector boson scattering and triboson production are unique probes of the possible high-energy dynamics underlying the Higgs potential. Furthermore, the different operators reflect directly in different energy dependencies of VBS and triboson production, and the study of these processes can not only detect the presence of new underlying dynamics but also distinguish between the operators through the differences in the kinematic shapes.

1.3.5 Multi-boson processes at HE pp colliders

Additional sensitivity studies have been performed using the Snowmass-DELPHES detector simulation. As mentioned earlier, the EFT operator $O_{\phi d}$ of Eq. 1.20 can be induced by a new heavy scalar coupling to the Higgs. This operator renormalizes the Higgs couplings to the gauge bosons and alters VBS. Using the $WZ \to 3\ell\nu$ final state in VBS mode, the sensitivity to this operator is quantified in Table 1-22.

Comparisons of sensitivity between 14 TeV and 33 TeV pp colliders are shown in Table 1-22 and 1-23. In VBS modes, the improvement for the dimension-6 operator is marginal but the dimension-8 operator gains

by a factor of two. With triboson production, the sensitivity improvement is even more impressive with a gain of a factor of 10.

Parameter	dimension	channel	Λ_{UV} [TeV]	300 fb^{-1}		3000 fb^{-1}	
				5σ	95% CL	5σ	95% CL
$c_{\phi d}/\Lambda^2$ at 14 TeV	6	WZ	1.9	29 TeV^{-2}	17 TeV^{-2}	15 TeV^{-2}	8.7 TeV^{-2}
$c_{\phi d}/\Lambda^2$ at 33 TeV	6	WZ	2.1	21 TeV^{-2}	13 TeV^{-2}	11 TeV^{-2}	6.6 TeV^{-2}

Table 1-22. *5σ-significance discovery values and 95% CL limits for coefficients of a dimension-6 operator. Λ_{UV} is the unitarity violation bound corresponding to the sensitivity wit h 3000 fb^{-1} of integrated luminosity.*

Parameter	channel	300 fb^{-1} at 14 TeV	3000 fb^{-1} at 14 TeV	3000 fb^{-1} at 33 TeV
$c_{\phi W}/\Lambda^2$	$ZZjj$	34 TeV^{-2}	16 TeV^{-2}	12 TeV^{-2}
f_{T1}/Λ^4	$WZjj$	1.3 TeV^{-4}	0.6 TeV^{-4}	0.3 TeV^{-4}
f_{T0}/Λ^4	WWW	1.2 TeV^{-4}	0.5 TeV^{-4}	0.05 TeV^{-4}

Table 1-23. *5σ-significance discovery values for coefficients of higher-dimension operators.*

1.3.6 Multi-boson processes at lepton colliders

1.3.7 aQGCs and new resonances

Authors: Juergen Reuter

1.3.8 TGCs from a global fit to Higgs data

Effective Lagrangians can be used to parametrize in a model independent way the low–energy effects of possible extensions of the standard model (SM) [85]. This bottom–up approach has the advantage of minimizing the amount of theoretical hypothesis when studying deviations from the SM predictions [86, 87]. Presently the observed Higgs–like state is consistent with being part of an electroweak scalar doublet, therefore, favoring that the $SU(2)_L \otimes U(1)_Y$ symmetry is linearly realized in the low–energy effective theory. In this scenario, the dimension–six operators $\mathcal{O}_6$ of Eq. 1.17 contain gauge–bosons, the Higgs doublet, and/or fermionic fields with couplings c_n. Here, Λ is a characteristic energy scale. There are 59 independent dimension–six operators up to flavor indices and Hermitian conjugation if we assume the conservation of baryon number [88, 89]. Notwithstanding, there is a freedom in the choice of the operator basis since operators connected by the equations of motion lead to the same S–matrix elements [90]. Taking advantage of the freedom in the choice of the operator basis, it is convenient to include in the basis used to analyze the Higgs couplings, operators that are directly related to the existing data, in particular to triple gauge couplings (TGCs), as well as, to the precision electroweak observables [86, 87, 100]. Neglecting, for the moment, modifications of the Higgs couplings to the first and second families and CP violating interactions, a useful basis is [87]

$$\mathcal{L}_{eff} = -\frac{\alpha_s v}{8\pi}\frac{f_g}{\Lambda^2}\mathcal{O}_{GG} + \frac{f_{WW}}{\Lambda^2}\mathcal{O}_{WW} + \frac{f_{\rm bot}}{\Lambda^2}\mathcal{O}_{d\Phi,33} + \frac{f_{\rm top}}{\Lambda^2}\mathcal{O}_{u\Phi,33} \tag{1.73}$$

$$+ \frac{f_\tau}{\Lambda^2}\mathcal{O}_{e\Phi,33} + \frac{f_W}{\Lambda^2}\mathcal{O}_W + \frac{f_B}{\Lambda^2}\mathcal{O}_B + \frac{f_{WWW}}{\Lambda^2}\mathcal{O}_{WWW}$$

with

$$\begin{aligned}
&\mathcal{O}_{GG} = \Phi^\dagger\Phi\, G^a_{\mu\nu}G^{a\mu\nu}\ ,\ \ \mathcal{O}_{WW} = \Phi^\dagger\hat{W}_{\mu\nu}\hat{W}^{\mu\nu}\Phi\ ,\\
&\mathcal{O}_W = (D_\mu\Phi)^\dagger\hat{W}^{\mu\nu}(D_\nu\Phi)\ ,\ \ \mathcal{O}_B = (D_\mu\Phi)^\dagger\hat{B}^{\mu\nu}(D_\nu\Phi)\ ,\\
&\mathcal{O}_{WWW} = \mathrm{Tr}[\hat{W}_{\mu\nu}\hat{W}^{\nu\rho}\hat{W}^{\mu}_{\rho}]\ ,\ \ \mathcal{O}_{u\Phi,ij} = (\Phi^\dagger\Phi)(\bar{L}_i\Phi u_{R_j})\ , \qquad (1.74)\\
&\mathcal{O}_{e\Phi,ij} = (\Phi^\dagger\Phi)(\bar{L}_i\Phi e_{R_j})\ ,\ \ \mathcal{O}_{d\Phi,ij} = (\Phi^\dagger\Phi)(\bar{Q}_i\Phi d_{Rj})\ ,
\end{aligned}$$

(1.75)

where Φ stands for the Higgs doublet with covariant derivative $D_\mu\Phi = \left(\partial_\mu + i\frac{1}{2}g'B_\mu + ig\frac{\sigma_a}{2}W^a_\mu\right)\Phi$ and $v = 246$ GeV is its vacuum expectation value. $\hat{B}_{\mu\nu} = i\frac{g'}{2}B_{\mu\nu}$ and $\hat{W}_{\mu\nu} = i\frac{g}{2}\sigma^a W^a_{\mu\nu}$ with $SU(2)_L$ ($U(1)_Y$) gauge coupling g (g') and Pauli matrices σ^a. We also use the notation of L for the lepton doublet, Q for the quark doublet and f_R for the $SU(2)$ singlet fermions, where i, j are flavor indices.

$\mathcal{O}_B$ and $\mathcal{O}_W$ contribute both to Higgs physics and TGCs which means that some changes of the couplings of the Higgs field to the vector gauge bosons are related to TGCs due to gauge invariance in a model independent fashion [100]. In fact, the TGCs γW^+W^- and ZW^+W^- can be parametrized as [102]

$$\mathcal{L}_{WWV} = -ig_{WWV}\Big\{g_1^V\left(W^+_{\mu\nu}W^{-\,\mu}V^\nu - W^+_\mu V_\nu W^{-\,\mu\nu}\right) + \kappa_V W^+_\mu W^-_\nu V^{\mu\nu} + \frac{\lambda_V}{m_W^2}W^+_{\mu\nu}W^{-\,\nu\rho}V_\rho{}^\mu\Big\}\ , \quad (1.76)$$

where $g_{WW\gamma} = e = gs$ and $g_{WWZ} = gc$ with $s(c)$ being the sine (cosine) of the weak mixing angle. In general these vertices involve six C and P conserving couplings [102]. Nevertheless, the electromagnetic gauge invariance requires that $g_1^\gamma = 1$, while the five remaining couplings are related to the dimension–six operators $\mathcal{O}_B$, $\mathcal{O}_W$ and $\mathcal{O}_{WWW}$

$$\Delta\kappa_\gamma = \frac{g^2v^2}{8\Lambda^2}\Big(f_W + f_B\Big)\ ,\ \lambda_\gamma = \lambda_Z = \frac{3g^2M_W^2}{2\Lambda^2}f_{WWW}\ ,\Delta g_1^Z = \frac{g^2v^2}{8c^2\Lambda^2}f_W\ ,\ \Delta\kappa_Z = \frac{g^2v^2}{8c^2\Lambda^2}\Big(c^2f_W - s^2f_B\Big)\ , \quad (1.77)$$

where we wrote $\kappa^V = 1 + \Delta\kappa^V$ and $g_1^Z = 1 + \Delta g_1^Z$.

1.3.8.1 Future perspective

Let us assess the impact of the Higgs physics in the TGC determination at the LHC with a center–of-mass energy of 14 TeV and an integrated luminosity of 300 fb^{-1}. In our first scenario we fit the ATLAS and CMS expected sensitivities [93, 94] for the Higgs signal strength using four independent parameters $\{f_g\ ,\ f_W\ ,\ f_B\ ,\ f_{WW}\}$ and setting the Yukawa couplings to the fermions to their SM values. This scenario captures most of the features of fits using a larger set of free parameters since the addittion of fermionic operators has little impact on the Higgs couplings to gauge–boson pairs and TGCs [86, 87].

Figure 1-14 displays $\Delta\chi^2$ as a function of the four fitting parameters [7]. We can observe in the left panel that the $\Delta\chi^2$ as a function of f_g exhibits two degenerate minima due to the interference between SM and anomalous contributions. In the case of the chi–square dependence on f_{WW} there is also an interference between anomalous and SM contributions, however, the degeneracy of the minima is lifted since the f_{WW} coupling contributes to Higgs decays into photons, WW^* and ZZ^*, as well as in Vh associated and vector boson fusion production mechanisms. Fig. 1-15 depicts the chi-square dependence on branching ratios and production cross sections. As we can see these quantities can be determined with a precision better than 20%.

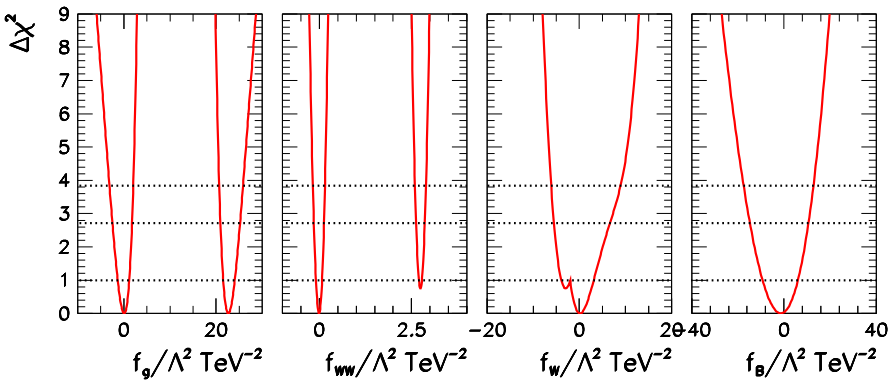

Figure 1-14. *$\Delta\chi^2$ as a function of f_g, f_{WW}, f_W, and f_B assuming $f_{\rm bot} = f_\tau = f_{\rm top} = 0$, after marginalizing over the three undisplayed ones. The three horizontal dashed lines stand for the $\Delta\chi^2$ values associated to 68%, 90% and 95% from bottom to top respectively.*

Now we focus our attention to the expected TGC bounds from Higgs data. Eq. (1.77) allows us to translate the constraints on f_W and f_B to bounds on $\Delta\kappa_\gamma$, $\Delta\kappa_Z$ and Δg_1^Z of which only two are independent. Fig 1-16 displays the result of our fit to the Higgs data where we plot the 90%, 95%, 99%, and 3σ CL allowed region in the plane $\Delta\kappa_\gamma \otimes \Delta g_1^Z$ after marginalizing over the other two parameters relevant to the Higgs analysis, *i.e.* f_g and f_{WW}. The expected 95% CL 1dof allowed ranges for the TGCs are

$$-0.029 \leq \Delta g_1^Z \leq 0.053\ , -0.067 \leq \Delta\kappa_\gamma \leq 0.067 \ \text{ which imply } \ -0.032 \leq \Delta\kappa_Z \leq 0.052 \tag{1.78}$$

Clearly the analysis of the Higgs data alone can improve the present best bounds on TGC which are still coming from LEP.

1.3.8.2 Discussion

Indirect new physics effects associated with extensions of the electroweak symmetry breaking sector can be written in terms of an effective Lagrangian whose lowest order operators are of dimension six. The coefficients of these dimension–six operators parametrize our ignorance of these effects. In the above framework changes of the couplings of the Higgs to electroweak gauge bosons are related to the anomalous triple gauge–boson vertices [95]. Therefore, the analysis of the Higgs boson data at LHC can be used to constrain TGCs. Moreover, the combination of future TGC and Higgs measurements have the potential to lead to the strongest constraints on new physics effects associated with this sector.

1.4 Conclusions

With the discovery of the Higgs boson and the measurement of its mass at the LHC, the last missing component of the SM has been determined. However, the big question related to the origin of the Higgs

[7] Details of the fitting procedure can be seen in Refs. [86, 87]

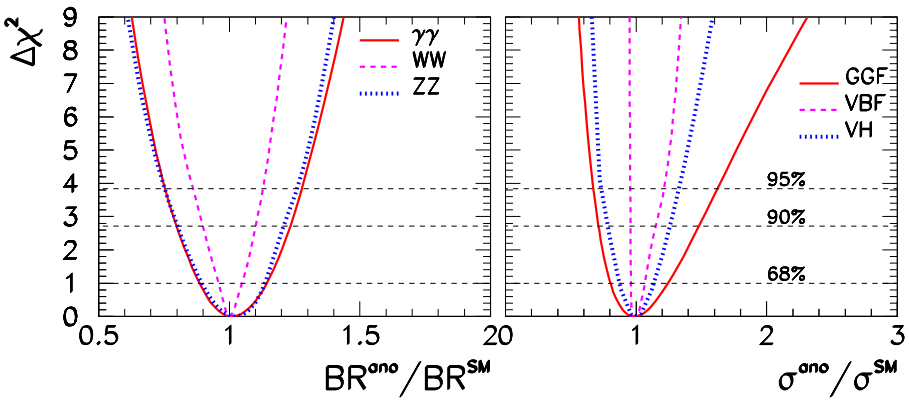

Figure 1-15. *Chi–square as a function of branching ratios (left panels) and production cross sections (right panels) when we use only the expected ATLAS and CMS sensitivity on the Higgs signal strengths.*

"mexican hat" potential remains to be answered. This question is exacerbated by the instability of this potential under quantum corrections.

The role of precision electroweak measurements is of increasing importance in over-constraining the Higgs sector of the SM. The two themes we have investigated in the arena of precision electroweak measurements are (a) the electroweak precision observables (EWPOs) that test the particle content and couplings in the SM and BSM scenarios, and (b) the measurements involving multiple gauge bosons in the final state which provide unique probes of the basic tenets of electroweak symmetry breaking.

In the case of EWPOs, we have focussed on the measurement of M_W and $\sin^2\theta^l_{\rm eff}$. Our conclusions are as follows:

- The knowledge of the Higgs mass has sharpened the predictions of these EWPOs such that the predictions are a factor of 2-4 more precise than the experimental measurements.
- In almost all extensions of the SM, which are associated with the electoweak symmetry-breaking sector, these EWPOs receive corrections due to quantum loops (due to e.g. supersymmetric particles or techni-fermions), or due to effective operators (induced for example in strongly-interacting light Higgs models), or due to Kaluza-Klein modes in extra-dimensional models.
- M_W and $\sin^2\theta^l_{\rm eff}$ typically have different sensitivities to the sources of new physics. This may be demonstrated by the parameterisation of new physics in the gauge boson self-energies in terms of the S, T and U "oblique" corrections. Fixed values of M_W and $\sin^2\theta^l_{\rm eff}$ correspond to lines in the $S-T$ plane with different slopes. Thus, improved measurements of both EWPOs can constrain all of the above sources of new physics in a relatively model-independent fashion.
- The current world average M_W has a precision of 15 MeV, dominated by the combined Tevatron measurement, which has a precision of 16 MeV based on the analysis of partial datasets. CDF and DO have projected that analyses of the full Tevatron statistics can yield a 10 MeV measurement, assuming a factor of two improvement in the uncertainty due to parton distribution functions, improvement in the calculation of radiative corrections and improved understanding of the trackers and calorimeters.

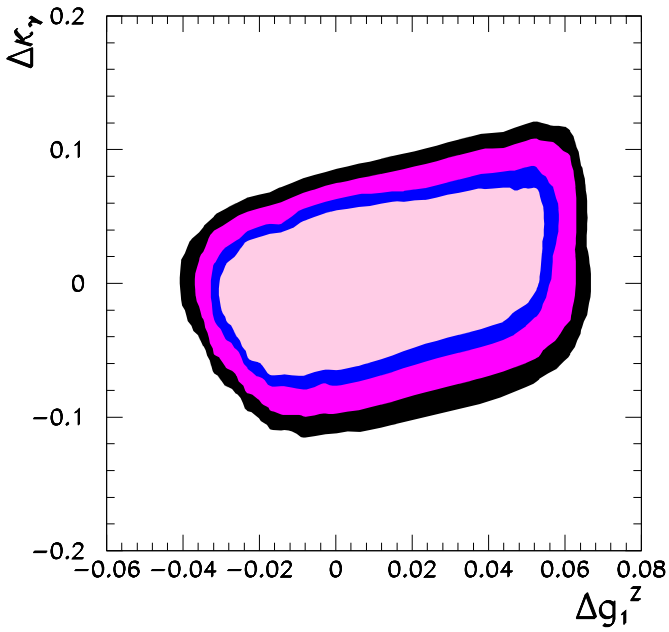

Figure 1-16. *We present the expected 90%, 95%, 99%, and 3σ allowed regions for the $\Delta\kappa_\gamma \otimes \Delta g_1^Z$ plane from the analysis of the Higgs data from LHC at 14 TeV with an integrated luminosity of 300 fb^{-1}.*

- Studies based on pseudo-data have demonstrated that measurements of boson distributions with the 2011-2012 LHC data may be able to improve the PDFs relevant for the M_W measurement by a factor of two in the near future, enabling the Tevatron potential for M_W to be realized.

- Enormous statisics of W bosons and control samples at the LHC offer the prospect of higher M_W precision. Studies based on pseudo-data have shown that the PDF uncertainty in M_W is about twice as big at the LHC as the Tevatron, due mainly to the larger fraction of sea quark-initiated production. Thus, further improvement by a factor of 2-3 in the PDFs will be required, beyond what is needed for the Tevatron. Furthermore, additional improvements in the QED radiative correction calculations and NNLO+NNLL generators for W and Z bosons will likely also be required. However, considering the 15-year time scale for the ultimate M_W measurement from the LHC, we consider a target precision of 5 MeV to be appropriate for the LHC.

- Studies of the M_W measurement at the ILC using the threshold scan and final state reconstruction have been updated. It is projected that the ILC will be able to perform the M_W measurement with a precision of 4-5 MeV.

- The circular electron-positron TLEP machine, running at the WW threshold, can produce very high statistics for the M_W measurement, and is likely to achieve energy calibration at the level of a fraction of an MeV. This potential motivates further studies of longitudinal beam polarization and control of other systematics achievable at TLEP. Given an integrated luminosity that can enable a statistical precision of ~ 0.5 MeV, further investigations of related issues are clearly warranted.

- The measurement of $\sin^2\theta_{\rm eff}$ from LEP and SLC have averaged to a precision of 16×10^{-5}, albeit with a $\sim 3\sigma$ difference between them. Additional, especially improved, measurements will be valuable to shed light on this difference.
- A measurement of $\sin^2\theta^l_{\rm eff}$ using the full Tevatron dataset is projected with a precision of 41×10^{-5}. This measurement will be interesting to compare with LEP and SLC.
- Compared to the Tevatron, measurement of $\sin^2\theta^l_{\rm eff}$ at the LHC is handicapped by a larger sensitivity to PDFs due to the dilution of the quark and antiquark directions. As with the M_W measurement, considerable control of the experimental and production model uncertainties will be required. Under the condition that a factor of 6-7 improvement on PDFs is achieved (a condition also required for the M_W target for the LHC), a projected uncertainty on $\sin^2\theta^l_{\rm eff}$ of 21×10^{-5} is obtained. This precision is similar to the current LEP and SLC measurements and is valuable before the advent of future lepton colliders.
- Considerably more precise measurements of $\sin^2\theta^l_{\rm eff}$ are highly desirable for taking the stringency of the SM tests to the next order of magnitude. Such measurements are possible at future lepton colliders running on the $Z-$pole such as ILC/GigaZ and TLEP.
- The ILC/GigaZ projection for the precision on $\sin^2\theta^l_{\rm eff}$ is 1.3×10^{-5}, a factor of 10 improvement on the current world average.
- Measurements of M_W at the few MeV level, and $\sin^2\theta^l_{\rm eff}$ at the level of 10^{-5}, require that the parametric uncertainties from m_{top} and α_{had} (the contribution to the running of α_{EM} from hadronic loops) as well as the missing higher order calculations be addressed. It is anticipated that calculations in the coming years will reduce the effect of missing higher-order calculations to a sub-dominant level. Parametric uncertainties from m_{top} and α_{had}, if reduced by a factor of two compared to current uncertainties, will prevent them from exceeding the total precision on M_W and $\sin^2\theta^l_{\rm eff}$. A factor of 3-4 improvement would be desirable, to $\delta m_{top}\sim0.3$ GeV and $\delta\alpha_{had}\sim0.3\times10^{-5}$. The LHC may be able to achieve $\delta m_{top}\sim0.5$ GeV but further progress at the LHC will likely be limited by theoretical uncertainties in the non-perturbative QCD effects associated with translating the kinematically-reconstructed m_{top} to the pole mass.
- TLEP may have the potential to go beyond ILC/GigaZ in the precision on $\sin^2\theta^l_{\rm eff}$, which also warrants a detailed study. In principle, the precision at TLEP could be high enough that all aspects of EWPOs, both theoretical and experimental, need to be revisited.

The second aspect of precision electroweak measurements we have emphasized is vector boson scattering and the related process of triboson production. Vector boson scattering addresses one of the crucial big questions that still remains open, ie. the unitarization of longitudinal vector boson scattering at high energy. In the SM, the unitarization is achieved when Higgs boson exchange amplitudes are included, and this mechanism relies on the longitudinal modes of the massive gauge bosons being the would-be Goldstone modes of the symmetry-breaking Higgs potential. A direct demonstration of this mechanism is required, and is a prime motivation for the HL-LHC.

Models which explain the lightness of the discovered Higgs boson by describing it as a pseudo-Goldstone boson associated with the breaking of a larger symmetry, often introduce higher-dimension operators as an effective field theory (EFT) approximation of the new dynamics. Testing for these operators in vector boson scattering and triboson production can answer one of the outstanding questions in the Higgs sector: is the dynamics associated with the stablization of the Higgs potential under quantum corrections, weakly coupled (e.g. SUSY) or strongly coupled (e.g. SILH models)?

The EFT formulation is not limited to specific models; any high energy theory can be reduced to a low-energy EFT and the former will specify the values of operator coefficients in the latter. Therefore, EFT operators provide a general method of parameterizing the effects of new physics at a high scale.

Some of these higher-dimension operators can alter the Higgs boson couplings, some can affect the values of EWPOs while others have no impact on these observables but still strongly affect multi-boson production. The study of the latter processes can provide direct evidence of new SILH dynamics through the energy-dependence of the anomalous production. Further clarification of the new dynamics can be provided by comparing final states involving different combinations of W and Z bosons and photons, which can elucidate the group structure of the new dynamics.

Our conclusions in the area of multi-boson production are as follows:

- Studies of vector boson scattering and triboson production have become possible, for the first time, at the LHC.
- For the next decade, the LHC will continue to be the facility to explore these processes at higher levels of precision.
- The HL-LHC is needed to demonstrate that the Higgs couplings to the electroweak vector bosons is an essential component of the unitarization mechanism for vector boson scattering. An integrated luminosity of 300 fb^{-1} is not enough.
- The sensitivity to higher-dimension operators improves by a factor of 2-3 with the HL-LHC, in comparison with the 300 fb^{-1} at the LHC.
- Triboson production is a particularly sensitive probe of higher dimension operators, complementary to vector boson scattering. This process becomes rapidly more sensitive with increasing beam energy, providing strong motivation for 33 TeV and 100 TeV pp colliders.
- Comparison to ILC for multi-boson production to be added.

ACKNOWLEDGEMENTS

References

[1] T. E. W. Group [CDF and D0 Collaborations], arXiv:1204.0042 [hep-ex].

[2] S. Heinemeyer, G. Weiglein and L. Zeune, DESY 13–015, *in preparation.*

[3] M. Frank, T. Hahn, S. Heinemeyer, W. Hollik, H. Rzehak and G. Weiglein, JHEP **0702** (2007) 047 [hep-ph/0611326].

[4] G. Degrassi, S. Heinemeyer, W. Hollik, P. Slavich and G. Weiglein, Eur. Phys. J. C **28** (2003) 133 [hep-ph/0212020].

[5] S. Heinemeyer, W. Hollik and G. Weiglein, Eur. Phys. J. C **9** (1999) 343 [hep-ph/9812472].

[6] S. Heinemeyer, W. Hollik and G. Weiglein, Comput. Phys. Commun. **124** (2000) 76 [hep-ph/9812320].

[7] T. Hahn, S. Heinemeyer, W. Hollik, H. Rzehak and G. Weiglein, Comput. Phys. Commun. **180** (2009) 1426.

[8] P. Bechtle, O. Brein, S. Heinemeyer, G. Weiglein and K. E. Williams, Comput. Phys. Commun. **181** (2010) 138 [arXiv:0811.4169 [hep-ph]].

[9] P. Bechtle, O. Brein, S. Heinemeyer, G. Weiglein and K. E. Williams, Comput. Phys. Commun. **182** (2011) 2605 [arXiv:1102.1898 [hep-ph]].

[10] S. Heinemeyer, W. Hollik, D. Stockinger, A. M. Weber and G. Weiglein, *JHEP* **0608** (2006) 052 [arXiv:hep-ph/0604147].

[11] S. Heinemeyer, O. Stål and G. Weiglein, Phys. Lett. B **710** (2012) 201 [arXiv:1112.3026 [hep-ph]];

[12] R. Barate *et al.* [LEP Working Group for Higgs boson searches and ALEPH and DELPHI and L3 and OPAL Collaborations], Phys. Lett. B **565** (2003) 61 [hep-ex/0306033].

[13] S. Schael *et al.* [ALEPH and DELPHI and L3 and OPAL and LEP Working Group for Higgs Boson Searches Collaborations], Eur. Phys. J. C **47** (2006) 547 [hep-ex/0602042].

[14] M. Carena, S. Heinemeyer, O. Stl, C. E. M. Wagner and G. Weiglein, arXiv:1302.7033 [hep-ph].

[15] A. Djouadi, Nuovo Cim. A **100**, 357 (1988);
B. A. Kniehl, Nucl. Phys. B **347**, 86 (1990);
A. Djouadi and P. Gambino, Phys. Rev. D **49**, 3499 (1994) [Erratum-ibid. D **53**, 4111 (1996)] [hep-ph/9309298];
M. Awramik, M. Czakon, A. Freitas, G. Weiglein, Phys. Rev. Lett. **93**, 201805 (2004) [hep-ph/0407317];
W. Hollik, U. Meier and S. Uccirati, Nucl. Phys. B **731**, 213 (2005) [hep-ph/0507158];
M. Awramik, M. Czakon and A. Freitas, Phys. Lett. B **642**, 563 (2006) [hep-ph/0605339];
W. Hollik, U. Meier and S. Uccirati, Nucl. Phys. B **765**, 154 (2007) [hep-ph/0610312].

[16] M. Awramik, M. Czakon and A. Freitas, JHEP **0611**, 048 (2006) [hep-ph/0608099].

[17] L. Avdeev, J. Fleischer, S. Mikhailov and O. Tarasov, Phys. Lett. B **336**, 560 (1994) [Erratum-ibid. B **349**, 597 (1994)] [hep-ph/9406363];
K. G. Chetyrkin, J. H. Kühn and M. Steinhauser, Phys. Lett. B **351**, 331 (1995) [hep-ph/9502291];
K. G. Chetyrkin, J. H. Kühn and M. Steinhauser, Phys. Rev. Lett. **75**, 3394 (1995) [hep-ph/9504413];
K. G. Chetyrkin, J. H. Kühn and M. Steinhauser, Nucl. Phys. B **482**, 213 (1996) [hep-ph/9606230].

[18] Y. Schröder and M. Steinhauser, Phys. Lett. B **622**, 124 (2005) [hep-ph/0504055];
K. G. Chetyrkin, M. Faisst, J. H. Kühn, P. Maierhoefer and C. Sturm, Phys. Rev. Lett. **97**, 102003 (2006) [hep-ph/0605201];
R. Boughezal and M. Czakon, Nucl. Phys. B **755**, 221 (2006) [hep-ph/0606232].

[19] J. J. van der Bij, K. G. Chetyrkin, M. Faisst, G. Jikia and T. Seidensticker, Phys. Lett. B **498**, 156 (2001) [hep-ph/0011373];
M. Faisst, J. H. Kühn, T. Seidensticker and O. Veretin, Nucl. Phys. B **665**, 649 (2003) [hep-ph/0302275].

[20] R. Boughezal, J. B. Tausk and J. J. van der Bij, Nucl. Phys. B **713**, 278 (2005) [hep-ph/0410216];
R. Boughezal, J. B. Tausk and J. J. van der Bij, Nucl. Phys. B **725**, 3 (2005) [hep-ph/0504092].

[21] M. Awramik, M. Czakon, A. Freitas and B. A. Kniehl, Nucl. Phys. B **813**, 174 (2009) [arXiv:0811.1364 [hep-ph]].

[22] A. Czarnecki and J. H. Kuhn, Phys. Rev. Lett. **77**, 3955 (1996) [hep-ph/9608366];
R. Harlander, T. Seidensticker and M. Steinhauser, Phys. Lett. B **426**, 125 (1998) [hep-ph/9712228].

[23] D. Y. Bardin, P. Christova, M. Jack, L. Kalinovskaya, A. Olchevski, S. Riemann and T. Riemann, Comput. Phys. Commun. **133**, 229 (2001) [hep-ph/9908433].

[24] M. Böhm and W. Hollik, Nucl. Phys. B **204**, 45 (1982);
S. Jadach, J. H. Kühn, R. G. Stuart and Z. Wąs, Z. Phys. C **38**, 609 (1988) [Erratum-ibid. C **45**, 528 (1990)].

[25] M. Greco, G. Pancheri-Srivastava and Y. Srivastava, Nucl. Phys. B **171**, 118 (1980) [Erratum-ibid. B **197**, 543 (1982)];
F. A. Berends, R. Kleiss and S. Jadach, Nucl. Phys. B **202**, 63 (1982).

[26] W. Hollik, *Predictions for e^+e^- Processes*, in *Precision Tests of the Standard Model*, ed. P. Langacker (World Scientific, Singapur, 1993), p. 117.

[27] A. Freitas and Y.-C. Huang, JHEP **1208**, 050 (2012) [arXiv:1205.0299 [hep-ph]].

[28] R. Barbieri, M. Beccaria, P. Ciafaloni, G. Curci and A. Vicere, Phys. Lett. B **288**, 95 (1992) [Erratum-ibid. B **312**, 511 (1993)] [hep-ph/9205238];
R. Barbieri, M. Beccaria, P. Ciafaloni, G. Curci and A. Vicere, Nucl. Phys. B **409**, 105 (1993);
J. Fleischer, O. V. Tarasov and F. Jegerlehner, Phys. Lett. B **319**, 249 (1993);
J. Fleischer, O. V. Tarasov and F. Jegerlehner, Phys. Rev. D **51**, 3820 (1995);
G. Degrassi and P. Gambino, Nucl. Phys. B **567**, 3 (2000) [hep-ph/9905472].

[29] A. B. Arbuzov, M. Awramik, M. Czakon, A. Freitas, M. W. Grünewald, K. Mönig, S. Riemann, T. Riemann, Comput. Phys. Commun. **174**, 728 (2006) [hep-ph/0507146].

[30] H. Flächer, M. Goebel, J. Haller, A. Höcker, K. Mönig and J. Stelzer, Eur. Phys. J. C **60**, 543 (2009) [Erratum-ibid. C **71**, 1718 (2011)] [arXiv:0811.0009 [hep-ph]].

[31] R. G. Stuart, Phys. Lett. B **262**, 113 (1991);
H. Veltman, Z. Phys. C **62**, 35 (1994).

[32] R. Hawkings and K. Mönig, EPJdirect C **8** (1999) 1 [arXiv:hep-ex/9910022].

[33] A. Blondel, Phys. Lett. B **202** (1988) 145 [Erratum-ibid. **208** (1988) 531].

[34] R. Hawkings and K. Monig, Eur. Phys. J. direct C **1** (1999) 8 [hep-ex/9910022].

[35] S. Heinemeyer, W. Hollik, A. M. Weber and G. Weiglein, JHEP **0804** (2008) 039 [arXiv:0710.2972 [hep-ph]].

[36] B. C. Allanach, M. Battaglia, G. A. Blair, M. S. Carena, A. De Roeck, A. Dedes, A. Djouadi and D. Gerdes *et al.*, Eur. Phys. J. C **25** (2002) 113 [hep-ph/0202233].

[37] S. Heinemeyer, S. Kraml, W. Porod and G. Weiglein, JHEP **0309** (2003) 075 [hep-ph/0306181].

[38] [Tevatron Electroweak Working Group and CDF and D0 Collaborations], arXiv:1107.5255 [hep-ex]; arXiv:1305.3929 [hep-ex].

[39] G. Weiglein *et al.* [LHC/LC Study Group Collaboration], Phys. Rept. **426** (2006) 47 [hep-ph/0410364].

[40] M. Davier, A. Hoecker, B. Malaescu and Z. Zhang, Eur. Phys. J. C **71**, 1515 (2011) [Erratum-ibid. C **72**, 1874 (2012)] [arXiv:1010.4180 [hep-ph]].

[41] K. Hagiwara, R. Liao, A. D. Martin, D. Nomura and T. Teubner, J. Phys. G **38**, 085003 (2011) [arXiv:1105.3149 [hep-ph]].

[42] M. Awramik, M. Czakon and A. Freitas, JHEP **0611**, 048 (2006) [hep-ph/0608099].

[43] M. Awramik, M. Czakon, A. Freitas and G. Weiglein, Phys. Rev. D **69**, 053006 (2004) [hep-ph/0311148].

[44] M. Steinhauser, Phys. Lett. B **429**, 158 (1998) [hep-ph/9803313].

[45] P. H. Chankowski, A. Dabelstein, W. Hollik, W. M. Mosle, S. Pokorski and J. Rosiek, Nucl. Phys. B **417**, 101 (1994).

[46] M. E. Peskin and T. Takeuchi, Phys. Rev. D **46**, 381 (1992).

[47] T. Corbett, O. J. P. Eboli, J. Gonzalez-Fraile and M. C. Gonzalez-Garcia, arXiv:1304.1151 [hep-ph].

[48] M. Baak, M. Goebel, J. Haller, A. Hoecker, D. Ludwig, K. Moenig, M. Schott and J. Stelzer, Eur. Phys. J. C **72**, 2003 (2012) [arXiv:1107.0975 [hep-ph]].

[49] T. Aaltonen *et al.* [CDF Collaboration], arXiv:1307.0770 [hep-ex].

[50] V. M. Abazov *et al.* [D0 Collaboration], Phys. Rev. D **84**, 012007 (2011) [arXiv:1104.4590 [hep-ex]].

[51] S. Chatrchyan *et al.* [CMS Collaboration], Phys. Rev. D **84**, 112002 (2011) [arXiv:1110.2682 [hep-ex]].

[52] The ATLAS collaboration, ATLAS-CONF-2013-043

[53] The ALEPH, DELPHI, L3, OPAL, SLD Collaborations, the LEP Electroweak Working Group, the SLD Electroweak and Heavy Flavour Groups, Phys. Rept. **427** 257, (2006) [hep-ex/0509008].

[54] T. Aaltonen *et al.* [CDF Collaboration], Phys. Rev. Lett. **106**, 241801 (2011) [arXiv:1103.5699 [hep-ex]]; V. M. Abazov *et al.* [DO Collaboration], Phys. Rev. D **84**, 012007 (2011) [arXiv:1104.4590 [hep-ex]].

[55] S. Chatrchyan *et al.* [CMS Collaboration], Phys. Lett. B **718**, 752 (2013) [arXiv:1207.3973 [hep-ex]]. G. Aad *et al.* [ATLAS Collaboration], ATLAS-CONF-2013-043.

[56] M. Awramik, M. Czakon, A. Freitas, G. Weiglein, Phys. Rev. Lett. **93**, 201805 (2004) [hep-ph/0407317]; M. Awramik, M. Czakon and A. Freitas, Phys. Lett. B **642**, 563 (2006) [hep-ph/0605339]; W. Hollik, U. Meier and S. Uccirati, Nucl. Phys. B **731**, 213 (2005) [hep-ph/0507158], Nucl. Phys. B **765**, 154 (2007) [hep-ph/0610312].

[57] M. Awramik, M. Czakon and A. Freitas, JHEP **0611**, 048 (2006) [hep-ph/0608099].

[58] L. Avdeev, J. Fleischer, S. Mikhailov and O. Tarasov, Phys. Lett. B **336**, 560 (1994) [Erratum-ibid. B **349**, 597 (1994)] [hep-ph/9406363];
K. G. Chetyrkin, J. H. Kühn and M. Steinhauser, Phys. Lett. B **351**, 331 (1995) [hep-ph/9502291];
K. G. Chetyrkin, J. H. Kühn and M. Steinhauser, Phys. Rev. Lett. **75**, 3394 (1995) [hep-ph/9504413];
K. G. Chetyrkin, J. H. Kühn and M. Steinhauser, Nucl. Phys. B **482**, 213 (1996) [hep-ph/9606230].

[59] Y. Schröder and M. Steinhauser, Phys. Lett. B **622**, 124 (2005) [hep-ph/0504055];
K. G. Chetyrkin, M. Faisst, J. H. Kühn, P. Maierhoefer and C. Sturm, Phys. Rev. Lett. **97**, 102003 (2006) [hep-ph/0605201];
R. Boughezal and M. Czakon, Nucl. Phys. B **755**, 221 (2006) [hep-ph/0606232].

[60] J. J. van der Bij, K. G. Chetyrkin, M. Faisst, G. Jikia and T. Seidensticker, Phys. Lett. B **498**, 156 (2001) [hep-ph/0011373];
M. Faisst, J. H. Kühn, T. Seidensticker and O. Veretin, Nucl. Phys. B **665**, 649 (2003) [hep-ph/0302275].

[61] R. Boughezal, J. B. Tausk and J. J. van der Bij, Nucl. Phys. B **713**, 278 (2005) [hep-ph/0410216], Nucl. Phys. B **725**, 3 (2005) [hep-ph/0504092].

[62] M. Awramik, M. Czakon, A. Freitas and B. A. Kniehl, Nucl. Phys. B **813**, 174 (2009) [arXiv:0811.1364 [hep-ph]].

[63] D. Y. Bardin, P. Christova, M. Jack, L. Kalinovskaya, A. Olchevski, S. Riemann and T. Riemann, Comput. Phys. Commun. **133**, 229 (2001) [hep-ph/9908433].

[64] M. Böhm and W. Hollik, Nucl. Phys. B **204**, 45 (1982);
S. Jadach, J. H. Kühn, R. G. Stuart and Z. Wąs, Z. Phys. C **38**, 609 (1988) [Erratum-ibid. C **45**, 528 (1990)].

[65] M. Greco, G. Pancheri-Srivastava and Y. Srivastava, Nucl. Phys. B **171**, 118 (1980) [Erratum-ibid. B **197**, 543 (1982)];
F. A. Berends, R. Kleiss and S. Jadach, Nucl. Phys. B **202**, 63 (1982).

[66] W. Hollik, *Predictions for e^+e^- Processes*, in *Precision Tests of the Standard Model*, ed. P. Langacker (World Scientific, Singapur, 1993), p. 117.

[67] A. Czarnecki and J. H. Kuhn, Phys. Rev. Lett. **77**, 3955 (1996) [hep-ph/9608366];
R. Harlander, T. Seidensticker and M. Steinhauser, Phys. Lett. B **426**, 125 (1998) [hep-ph/9712228].

[68] A. Freitas and Y.-C. Huang, JHEP **1208**, 050 (2012) [arXiv:1205.0299 [hep-ph]].

[69] R. Barbieri, M. Beccaria, P. Ciafaloni, G. Curci and A. Vicere, Phys. Lett. B **288**, 95 (1992) [Erratum-ibid. B **312**, 511 (1993)] [hep-ph/9205238];
R. Barbieri, M. Beccaria, P. Ciafaloni, G. Curci and A. Vicere, Nucl. Phys. B **409**, 105 (1993);
J. Fleischer, O. V. Tarasov and F. Jegerlehner, Phys. Lett. B **319**, 249 (1993);
J. Fleischer, O. V. Tarasov and F. Jegerlehner, Phys. Rev. D **51**, 3820 (1995);
G. Degrassi and P. Gambino, Nucl. Phys. B **567**, 3 (2000) [hep-ph/9905472].

[70] T. van Ritbergen and R. G. Stuart, Phys. Rev. Lett. **82**, 488 (1999) [hep-ph/9808283];
M. Steinhauser and T. Seidensticker, Phys. Lett. B **467**, 271 (1999) [hep-ph/9909436].

[71] A. Freitas, W. Hollik, W. Walter and G. Weiglein, Phys. Lett. B **495**, 338 (2000) [Erratum-ibid. B **570**, 260 (2003)] [hep-ph/0007091];
M. Awramik and M. Czakon, Phys. Rev. Lett. **89**, 241801 (2002) [hep-ph/0208113];
A. Onishchenko and O. Veretin, Phys. Lett. B **551**, 111 (2003) [hep-ph/0209010];
M. Awramik and M. Czakon, Phys. Lett. B **568**, 48 (2003) [hep-ph/0305248].

[72] M. Awramik, M. Czakon, A. Freitas and G. Weiglein, Phys. Rev. D **69**, 053006 (2004) [hep-ph/0311148].

[73] A. B. Arbuzov, M. Awramik, M. Czakon, A. Freitas, M. W. Grünewald, K. Mönig, S. Riemann, T. Riemann, Comput. Phys. Commun. **174**, 728 (2006) [hep-ph/0507146].

[74] H. Flächer, M. Goebel, J. Haller, A. Höcker, K. Mönig and J. Stelzer, Eur. Phys. J. C **60**, 543 (2009) [Erratum-ibid. C **71**, 1718 (2011)] [arXiv:0811.0009 [hep-ph]].

[75] R. G. Stuart, Phys. Lett. B **262**, 113 (1991);
H. Veltman, Z. Phys. C **62**, 35 (1994).

[76] M. Davier, A. Hoecker, B. Malaescu and Z. Zhang, Eur. Phys. J. C **71**, 1515 (2011) [Erratum-ibid. C **72**, 1874 (2012)] [arXiv:1010.4180 [hep-ph]].

[77] K. Hagiwara, R. Liao, A. D. Martin, D. Nomura and T. Teubner, J. Phys. G **38**, 085003 (2011) [arXiv:1105.3149 [hep-ph]].

[78] The Tevatron Electroweak Working Group and the CDF and DO Collaborations, arXiv:1107.5255 [hep-ex].

[79] J. Beringer *et al.* [Particle Data Group Collaboration], Phys. Rev. D **86**, 010001 (2012).

[80] M. E. Peskin and T. Takeuchi, Phys. Rev. D **46**, 381 (1992).

[81] A. Bodek, Eur.Phys.J.C67:321 (2010), arXiv:0911.2850 [hep-ex]

[82] A. Bodek et. al. , Eur.Phys.J.C72: 2194 (2012), arXiv:1208.3710 [hep-ex]

[83] J. Collins and D. Soper, Phys. Rev. **D16**, 2219 (1977).

[84] M. Baak, M. Goebel, J. Haller, A. Hoecker, D. Kennedy, R. Kogler, K. Moenig and M. Schott *et al.*, Eur. Phys. J. C **72**, 2205 (2012) [arXiv:1209.2716 [hep-ph]].

[85] S. Weinberg, Physica A **96**, 327 (1979).

[86] T. Corbett, O. J. P. Eboli, J. Gonzalez-Fraile and M. C. Gonzalez-Garcia, Phys. Rev. D **87**, 015022 (2013) [arXiv:1211.4580 [hep-ph]].

[87] T. Corbett, O. J. P. Eboli, J. Gonzalez-Fraile and M. C. Gonzalez-Garcia, Phys. Rev. D **86**, 075013 (2012) [arXiv:1207.1344 [hep-ph]].

[88] W. Buchmuller and D. Wyler, Phys. Lett. B **177**, 377 (1986).

[89] B. Grzadkowski, M. Iskrzynski, M. Misiak and J. Rosiek, JHEP **1010**, 085 (2010) [arXiv:1008.4884 [hep-ph]].

[90] H. D. Politzer, Nucl. Phys. B **172**, 349 (1980); H. Georgi, Nucl. Phys. B **361**, 339 (1991); C. Arzt, Phys. Lett. B **342**, 189 (1995); H. Simma, Z. Phys. C **61**, 67 (1994).

[91] T. Corbett, O. J. P. Eboli, J. Gonzalez-Fraile and M. C. Gonzalez-Garcia, Phys. Rev. Letters **111**, 011801 (2013) [arXiv:1304.1151 [hep-ph]].

[92] K. Hagiwara, R. Peccei, D. Zeppenfeld, and K. Hikasa, Nucl. Phys. **B282**, 253 (1987).

[93] ATLAS collaboration, ATL-PHYS-PUB-2012-004.

[94] CMS collaboration, `https://twiki.cern.ch/twiki/bin/view/CMSPublic/HigProjectionEsg2012TWiki`

[95] For an early application of this framework to the Tevatron data see F. de Campos, M. C. Gonzalez-Garcia and S. F. Novaes, Phys. Rev. Lett. **79**, 5210 (1997) [hep-ph/9707511].

[96] G. Bozzi, F. Campanario, C. NEnglert, M. Rauch, M. Spannoswky and D. Zeppenfeld, arXiv:1205.2506 [hep-ph].

[97] W. Kilian, T. Ohl and J. Reuter, Eur. Phys. J. C **71**, 1742 (2011) [arXiv:0708.4233 [hep-ph]].

[98] N. D. Christensen, C. Duhr, B. Fuks, J. Reuter and C. Speckner, Eur. Phys. J. C **72**, 1990 (2012) [arXiv:1010.3251 [hep-ph]].

[99] C. Degrande, N. Greiner, W. Kilian, O. Mattelaer, H. Mebane, T. Stelzer, S. Willenbrock and C. Zhang, arXiv:1205.4231 [hep-ph].

[100] T. Corbett, O. J. P. Eboli, J. Gonzalez-Fraile and M. C. Gonzalez-Garcia, arXiv:1304.1151 [hep-ph].

[101] K. Hagiwara, S. Ishihara, R. Szalapski and D. Zeppenfeld, Phys. Rev. D **48**, 2182 (1993).

[102] K. Hagiwara, R. D. Peccei, D. Zeppenfeld and K. Hikasa, Nucl. Phys. B **282**, 253 (1987).

[103] B. Grzadkowski, M. Iskrzynski, M. Misiak and J. Rosiek, JHEP **1010**, 085 (2010) [arXiv:1008.4884 [hep-ph]].

[104] J. Wudka, Int. J. Mod. Phys. A **9**, 2301 (1994) [hep-ph/9406205].

[105] O. J. P. Eboli, M. C. Gonzalez-Garcia and J. K. Mizukoshi, "$pp \to jje^{\pm}\mu^{\mp}\nu\nu$ and $jje^{\pm}\mu^{\mp}\nu\nu$ at $\mathcal{O}(\alpha^{\not{}}_{\updownarrow})$ and $\mathcal{O}(\alpha_{em}^4\alpha_s^2)$ for the study of the quartic electroweak gauge boson vertex at CERN LHC," Phys. Rev. D **74**, 073005 (2006) [hep-ph/0606118].

[106] C. Arzt, M. B. Einhorn and J. Wudka, Nucl. Phys. B **433**, 41 (1995) [hep-ph/9405214].

[107] See for instance, and references therein, http://pdg.lbl.gov/2010/reviews/rpp2010-rev-wz-quartic-couplings.pdf.

[108] K. Arnold, J. Bellm, G. Bozzi, F. Campanario, C. Englert, et al., *Release Note – VBFNLO-2.6.0*, `arXiv:1207.4975 [hep-ph]`.

[109] K. Arnold, J. Bellm, G. Bozzi, M. Brieg, F. Campanario, et al., *VBFNLO: A parton level Monte Carlo for processes with electroweak bosons – Manual for Version 2.5.0*, `arXiv:1107.4038 [hep-ph]`.

[110] K. Arnold et al., *VBFNLO: A parton level Monte Carlo for processes with electroweak bosons*, Comput. Phys. Commun. **180** (2009) 1661–1670, `arXiv:0811.4559 [hep-ph]`.

[111] M. R. Whalley, D. Bourilkov and R. C. Group, hep-ph/0508110.

[112] J. Alwall, A. Ballestrero, P. Bartalini, S. Belov, E. Boos, A. Buckley, J. M. Butterworth and L. Dudko *et al.*, Comput. Phys. Commun. **176**, 300 (2007) [hep-ph/0609017].

[113] M. Dobbs and J. B. Hansen, Comput. Phys. Commun. **134**, 41 (2001).

[114] V. D. Barger, K. -m. Cheung, T. Han and R. J. N. Phillips, Phys. Rev. D **42**, 3052 (1990).

[115] U. Baur and D. Zeppenfeld, Phys. Lett. B **201**, 383 (1988).

[116] U. Baur and D. Zeppenfeld, Nucl. Phys. B **308**, 127 (1988).

[117] G. J. Gounaris, J. Layssac and F. M. Renard, Phys. Lett. B **332**, 146 (1994) [hep-ph/9311370].

[118] G. J. Gounaris, J. Layssac, J. E. Paschalis and F. M. Renard, Z. Phys. C **66**, 619 (1995) [hep-ph/9409260].

[119] http://www.itp.kit.edu/ vbfnloweb/wiki/doku.php?id=download:formfactor

[120] B. Jager, C. Oleari and D. Zeppenfeld, JHEP **0607**, 015 (2006) [hep-ph/0603177].

[121] B. Jager, C. Oleari and D. Zeppenfeld, Phys. Rev. D **73**, 113006 (2006) [hep-ph/0604200].

[122] G. Bozzi, B. Jager, C. Oleari and D. Zeppenfeld, Phys. Rev. D **75**, 073004 (2007) [hep-ph/0701105].

[123] B. Jager, C. Oleari and D. Zeppenfeld, Phys. Rev. D **80**, 034022 (2009) [arXiv:0907.0580 [hep-ph]].

[124] A. Lazopoulos, K. Melnikov and F. Petriello, Phys. Rev. D **76**, 014001 (2007) [hep-ph/0703273].

[125] V. Hankele and D. Zeppenfeld, Phys. Lett. B **661**, 103 (2008) [arXiv:0712.3544 [hep-ph]].

[126] F. Campanario, V. Hankele, C. Oleari, S. Prestel and D. Zeppenfeld, Phys. Rev. D **78**, 094012 (2008) [arXiv:0809.0790 [hep-ph]].

[127] T. Binoth, G. Ossola, C. G. Papadopoulos and R. Pittau, JHEP **0806**, 082 (2008) [arXiv:0804.0350 [hep-ph]].

[128] G. Bozzi, F. Campanario, V. Hankele and D. Zeppenfeld, Phys. Rev. D **81**, 094030 (2010) [arXiv:0911.0438 [hep-ph]].

[129] G. Bozzi, F. Campanario, M. Rauch, H. Rzehak and D. Zeppenfeld, Phys. Lett. B **696**, 380 (2011) [arXiv:1011.2206 [hep-ph]].

[130] U. Baur, D. Wackeroth and M. M. Weber, PoS RADCOR **2009**, 067 (2010) [arXiv:1001.2688 [hep-ph]].

[131] G. Bozzi, F. Campanario, M. Rauch and D. Zeppenfeld, Phys. Rev. D **83**, 114035 (2011) [arXiv:1103.4613 [hep-ph]].

[132] G. Bozzi, F. Campanario, M. Rauch and D. Zeppenfeld, Phys. Rev. D **84**, 074028 (2011) [arXiv:1107.3149 [hep-ph]].

[133] J. M. Campbell, H. B. Hartanto and C. Williams, JHEP **1211**, 162 (2012) [arXiv:1208.0566 [hep-ph]].

[134] R. W. Brown, K. L. Kowalski and S. J. Brodsky, Phys. Rev. D **28**, 624 (1983).

[135] U. Baur, T. Han and J. Ohnemus, Phys. Rev. D **48**, 5140 (1993) [hep-ph/9305314].

[136] U. Baur, T. Han, N. Kauer, R. Sobey and D. Zeppenfeld, Phys. Rev. D **56**, 140 (1997) [hep-ph/9702364].

[137] J. Pumplin, D. R. Stump, J. Huston, H. L. Lai, P. M. Nadolsky and W. K. Tung, JHEP **0207**, 012 (2002) [hep-ph/0201195].

[138] http://feynrules.irmp.ucl.ac.be/wiki/AnomalousGaugeCoupling

[139] "Precision measurement of the W mass with a polarized threshold scan at a linear collider." G. W. Wilson. In *2nd ECFA/DESY Study 1998-2001* 1498-1505 LC-PHSM-2001-09 and in Proceedings of LCWS 1999, Sitges, Spain.

[140] "Investigating In-Situ Center-of-Mass Energy Determination with Di-Muon Events", G. W. Wilson, ECFA LC2013 Workshop, Hamburg, May2013.

[141] S. Schael *et al.* [ALEPH and DELPHI and L3 and OPAL and LEP Electroweak Working Group Collaborations], "Electroweak Measurements in Electron-Positron Collisions at W-Boson-Pair Energies at LEP," arXiv:1302.3415 [hep-ex].

[142] M. Beckmann, B. List and J. List, "Treatment of Photon Radiation in Kinematic Fits at Future e+ e- Colliders," Nucl. Instrum. Meth. A **624**, 184 (2010) [arXiv:1006.0436 [hep-ex]].

[143] S. Heinemeyer, G. Weiglein and L. Zeune, DESY 13–015, *in preparation.*

[144] M. Frank, T. Hahn, S. Heinemeyer, W. Hollik, H. Rzehak and G. Weiglein, JHEP **0702** (2007) 047 [hep-ph/0611326].

[145] G. Degrassi, S. Heinemeyer, W. Hollik, P. Slavich and G. Weiglein, Eur. Phys. J. C **28** (2003) 133 [hep-ph/0212020].

[146] S. Heinemeyer, W. Hollik and G. Weiglein, Eur. Phys. J. C **9** (1999) 343 [hep-ph/9812472].

[147] S. Heinemeyer, W. Hollik and G. Weiglein, Comput. Phys. Commun. **124** (2000) 76 [hep-ph/9812320].

[148] T. Hahn, S. Heinemeyer, W. Hollik, H. Rzehak and G. Weiglein, Comput. Phys. Commun. **180** (2009) 1426.

[149] P. Bechtle, O. Brein, S. Heinemeyer, G. Weiglein and K. E. Williams, Comput. Phys. Commun. **181** (2010) 138 [arXiv:0811.4169 [hep-ph]].

[150] P. Bechtle, O. Brein, S. Heinemeyer, G. Weiglein and K. E. Williams, Comput. Phys. Commun. **182** (2011) 2605 [arXiv:1102.1898 [hep-ph]].

[151] S. Heinemeyer, W. Hollik, D. Stockinger, A. M. Weber and G. Weiglein, *JHEP* **0608** (2006) 052 [arXiv:hep-ph/0604147].

[152] S. Heinemeyer, W. Hollik, A. M. Weber and G. Weiglein, JHEP **0804** (2008) 039 [arXiv:0710.2972 [hep-ph]].

[153] S. Heinemeyer, O. Stål and G. Weiglein, Phys. Lett. B **710** (2012) 201 [arXiv:1112.3026 [hep-ph]];

[154] R. Barate *et al.* [LEP Working Group for Higgs boson searches and ALEPH and DELPHI and L3 and OPAL Collaborations], Phys. Lett. B **565** (2003) 61 [hep-ex/0306033].

[155] S. Schael *et al.* [ALEPH and DELPHI and L3 and OPAL and LEP Working Group for Higgs Boson Searches Collaborations], Eur. Phys. J. C **47** (2006) 547 [hep-ex/0602042].

[156] M. Carena, S. Heinemeyer, O. Stl, C. E. M. Wagner and G. Weiglein, arXiv:1302.7033 [hep-ph].

[157] A. Denner, S. Dittmaier, M. Roth and D. Wackeroth, Phys. Lett. B **475**, 127 (2000) [hep-ph/9912261]; Nucl. Phys. B **587**, 67 (2000) [hep-ph/0006307].

[158] S. Jadach, W. Placzek, M. Skrzypek, B. F. L. Ward and Z. Was, Phys. Rev. D **65**, 093010 (2002) [hep-ph/0007012].

[159] A. Denner, S. Dittmaier, M. Roth and L. H. Wieders, Phys. Lett. B **612**, 223 (2005) [Erratum-ibid. B **704**, 667 (2011)] [hep-ph/0502063]; Nucl. Phys. B **724**, 247 (2005) [Erratum-ibid. B **854**, 504 (2012)] [hep-ph/0505042].

[160] V. S. Fadin, L. N. Lipatov, A. D. Martin and M. Melles, Phys. Rev. D **61**, 094002 (2000) [hep-ph/9910338]; A. Denner, M. Melles and S. Pozzorini, Nucl. Phys. B **662**, 299 (2003) [hep-ph/0301241]; M. Beccaria, F. M. Renard and C. Verzegnassi, Nucl. Phys. B **663**, 394 (2003) [hep-ph/0304175].

[161] J. H. Kühn, F. Metzler and A. A. Penin, Nucl. Phys. B **795**, 277 (2008) [Erratum-ibid. **818**, 135 (2009)] [arXiv:0709.4055 [hep-ph]].

[162] V. S. Fadin, V. A. Khoze, A. D. Martin and W. J. Stirling, Phys. Lett. **B363**, 112 (1995).

[163] S. Actis, M. Beneke, P. Falgari and C. Schwinn, Nucl. Phys. B **807**, 1 (2009) [arXiv:0807.0102 [hep-ph]].

[164] M. Beneke, P. Falgari, C. Schwinn, A. Signer and G. Zanderighi, Nucl. Phys. B **792**, 89 (2008) [arXiv:0707.0773 [hep-ph]].

[165] M. Skrzypek, Acta Phys. Polon. **B23**, 135 (1992).

[166] V. Lombardo [on behalf of the ATLAS and CMS Collaboration], arXiv:1305.3773 [hep-ex].

[167] A. V. Kotwal and J. Stark, Ann. Rev. Nucl. Part. Sci. **58**, 147 (2008).

[168] C. Balazs and C. P. Yuan, Phys. Rev. D **56**, 5558 (1997) [arXiv:hep-ph/9704258]; R. K. Ellis and S. Veseli, Nucl. Phys. B **511**, 649 (1998) [arXiv:hep-ph/9706526].

[169] F. Landry, R. Brock, G. Ladinsky and C. P. Yuan, Phys. Rev. D **63**, 013004 (2001) [arXiv:hep-ph/9905391].

[170] S. Frixione and B. R. Webber, JHEP **0206**, 029 (2002) [arXiv:hep-ph/0204244]; S. Frixione, F. Stoeckli, P. Torrielli, B. R. Webber and C. D. White, [arXiv:hep-ph/1010.0819].

[171] S. Alioli, P. Nason, C. Oleari and E. Re, JHEP **0807**, 060 (2008) [arXiv:hep-ph/0805.4802].

[172] K. Hamilton, P. Richardson and J. Tully, JHEP **0810**, 015 (2008) [arXiv:0806.0290 [hep-ph]]

[173] C. Anastasiou, L. J. Dixon, K. Melnikov and F. Petriello, Phys. Rev. D **69**, 094008 (2004) [arXiv:hep-ph/0312266].

[174] K. Melnikov and F. Petriello, Phys. Rev. Lett. **96**, 231803 (2006) [arXiv:hep-ph/0603182].

[175] S. Catani, L. Cieri, G. Ferrera, D. de Florian and M. Grazzini, Phys. Rev. Lett. **103**, 082001 (2009) [arXiv:0903.2120 [hep-ph]].

[176] F. Abe *et al.* [CDF Collaboration], Phys. Rev. Lett. **75**, 11 (1995) and Phys. Rev. D **52**, 4784 (1995); T. Affolder *et al.* [CDF Collaboration], Phys. Rev. D **64**, 052001 (2001).

[177] S. Abachi *et al.* [D0 Collaboration], Phys. Rev. Lett. **77**, 3309 (1996), B. Abbott *et al.* [D0 Collaboration], Phys. Rev. D **58**, 012002 (1998); Phys. Rev. D **58**, 092003 (1998); Phys. Rev. Lett. **80**, 3008 (1998); Phys. Rev. Lett. **84**, 222 (2000); Phys. Rev. D **62** 092006 (2000); V. M. Abazov *et al.* [D0 Collaboration], Phys. Rev. D **66**, 012001 (2002).

[178] W. Ashmanskas *et al.* [TEVEWWG], arXiv:hep-ex/0311039 and references therein.

[179] F. Abe *et al.* [CDF Collaboration], Phys. Rev. Lett. **74**, 341 (1995).

[180] T. Affolder *et al.* [CDF Collaboration], Phys. Rev. Lett. **85**, 3347 (2000).

[181] V. M. Abazov *et al.* [D0 Collaboration], Phys. Rev. D **66**, 032008 (2002).

[182] D. Wackeroth and W. Hollik, Phys. Rev. D **55**, 6788 (1997) [arXiv:hep-ph/9606398].

[183] U. Baur, S. Keller and D. Wackeroth, Phys. Rev. D **59**, 013002 (1999) [arXiv:hep-ph/9807417].

[184] S. Dittmaier and M. 1. Kramer, Phys. Rev. D **65**, 073007 (2002) [arXiv:hep-ph/0109062].

[185] U. Baur and D. Wackeroth, Phys. Rev. D **70**, 073015 (2004) [arXiv:hep-ph/0405191].

[186] A. Arbuzov, D. Bardin, S. Bondarenko, P. Christova, L. Kalinovskaya, G. Nanava and R. Sadykov, Eur. Phys. J. C **46**, 407 (2006) [Erratum-ibid. C **50**, 505 (2007)] [arXiv:hep-ph/0506110].

[187] C. M. Carloni Calame, G. Montagna, O. Nicrosini and A. Vicini, JHEP **0612**, 016 (2006) [arXiv:hep-ph/0609170].

[188] V. A. Zykunov, Phys. Atom. Nucl. **71**, 732 (2008); Eur. Phys. J. direct C **3**, 9 (2001) [arXiv:hep-ph/0107059].

[189] C. Buttar *et al.*, [arXiv:hep-ph/0604120.]

[190] C. E. Gerber *et al.* [TeV4LHC-Top and Electroweak Working Group], [arXiv:hep-ph/0705.3251].

[191] C. M. Carloni Calame, G. Montagna, O. Nicrosini and M. Treccani, Phys. Rev. D **69**, 037301 (2004).

[192] W. Placzek and S. Jadach, Eur. Phys. J. C **29**, 325 (2003).

[193] P. Golonka and Z. Was, Eur. Phys. J. C **45**, 97 (2006) [arXiv:hep-ph/0506026].

[194] K. Hamilton and P. Richardson, JHEP **0607**, 010 (2006) [arXiv:hep-ph/0603034].

[195] S. Brensing, S. Dittmaier, M. 1. Kramer and A. Muck, Phys. Rev. D **77**, 073006 (2008) [arXiv:0710.3309 [hep-ph]].

[196] E. Laenen and D. Wackeroth, Ann. Rev. Nucl. Part. Sci. **59**, 367 (2009).

[197] Q. H. Cao and C. P. Yuan, Phys. Rev. Lett. **93**, 042001 (2004) [arXiv:hep-ph/0401026].

[198] G. Balossini *et al.*, JHEP **1001**, 013 (2010) [arXiv:hep-ph/0907.0276].

[199] G. Corcella, I. G. Knowles, G. Marchesisni, S. Moretti, K. Odagiri, P. Richardson, M. H. Seymour and B. R. Webber, JHEP **0101**, 010 (2001) [arXiv:hep-ph/0011363, hep-ph/0210213]

[200] A. Arbuzov, D. Bardin, S. Bondarenko, P. Christova, L. Kalinovskaya, G. Nanava, R. Sadykov, Eur. Phys. J. C **54**, 451 (2008) [arXiv:0711.0625 [hep-ph]].

[201] T. Sjostrand, S. Mrenna and P. Z. Skands, JHEP **0605**, 026 (2006) [hep-ph/0603175]

[202] P. Richardson, R. R. Sadykov, A. A. Sapronov, M. H. Seymour and P. Z. Skands, arXiv:1011.5444 [hep-ph].

[203] P. Nason, JHEP **0411**, 040 (2004) [arXiv:hep-ph/0409146].

[204] S. Frixione, P. Nason and C. Oleari, JHEP **0711**, 070 (2007) [arXiv:hep-ph/0709.2092].

[205] S. Alioli, P. Nason, C. Oleari and E. Re, JHEP **1006**, 043 (2010) [arXiv:1002.2581 [hep-ph]].

[206] C. Bernaciak and D. Wackeroth, Phys. Rev. D **85**, 093003 (2012) [arXiv:1201.4804 [hep-ph]].

[207] L. Barze, G. Montagna, P. Nason, O. Nicrosini and F. Piccinini, JHEP **1204**, 037 (2012) [arXiv:1202.0465 [hep-ph]].

[208] L. Barze', G. Montagna, P. Nason, O. Nicrosini, F. Piccinini and A. Vicini, Eur. Phys. J. C **73**, 2474 (2013) [arXiv:1302.4606 [hep-ph]].

[209] G. Bozzi, J. Rojo and A. Vicini, Phys. Rev. D **83**, 113008 (2011) [arXiv:1104.2056 [hep-ph]].